

CONVEX BICLUSTERING

BY ERIC C. CHI, GENEVERA I. ALLEN AND RICHARD G. BARANIUK

Rice University

In the biclustering problem, we seek to simultaneously group observations and features. While biclustering has applications in a wide array of domains, ranging from text mining to collaborative filtering, the problem of identifying structure in high dimensional genomic data motivates this work. In this context, biclustering enables us to identify subsets of genes that are co-expressed only within a subset of experimental conditions. We present a convex formulation of the biclustering problem that possesses a unique global minimizer and an iterative algorithm, COBRA, that is guaranteed to identify it. Our approach generates an entire solution path of possible biclusters as a single tuning parameter is varied. We also show how to reduce the problem of selecting this tuning parameter to solving a trivial modification of the convex biclustering problem. The key contributions of our work are its simplicity, interpretability, and algorithmic guarantees - features that arguably are lacking in the current alternative algorithms. We demonstrate the advantages of our approach, which includes stably and reproducibly identifying biclusterings, on simulated and real microarray data.

1. Introduction. In the biclustering problem, we seek to simultaneously group observations (columns) and features (rows) in a data matrix. Such data is sometimes described as two-way, or transposable, to put the rows and columns on equal footing and to emphasize the desire to uncover structure in both the row and column variables. Biclustering is used for visualization and exploratory analysis in a wide array of domains. For example, in text mining, biclustering can identify subgroups of documents with similar properties with respect to a subgroup of words (Dhillon, 2001). In collaborative filtering, it can be used to identify subgroups of customers with similar preferences for a subset of products (Hofmann and Puzicha, 1999). Comprehensive reviews of biclustering methods can be found in (Madeira and Oliveira, 2004; Tanay, Sharan and Shamir, 2005; Busygin, Prokopyev and Pardalos, 2008).

In this work, we focus on biclustering to identify patterns in high dimensional cancer genomic data. While a cancer, such as breast cancer, may present clinically as a homogenous disease, it typically consists of several distinct subtypes at the molecular level. A fundamental goal of cancer research is the identification of subtypes of cancerous tumors that have similar molecular profiles and the genes that characterize each of the subtypes. Identifying these patterns is the first step towards developing personalized treatment strategies targeted to a patient's particular cancer subtype.

Subtype discovery can be posed as a biclustering problem in which gene expression data is partitioned into a checkerboard-like pattern that highlights the associations between groups of patients and groups of genes that distinguish those patients. Biclustering has had some notable successes in subtype discovery. For instance, biclustering breast cancer data has identified sets of genes whose expression levels segregated patients into five subtypes with distinct survival outcomes (Sørlie et al., 2001). These subtypes have been reproduced in numerous studies (Sørlie et al., 2003). Encouraged by these results,

Keywords and phrases: Clustering, Convex Optimization, Fused Lasso, Gene Expression, Reproducible Research, Structured Sparsity

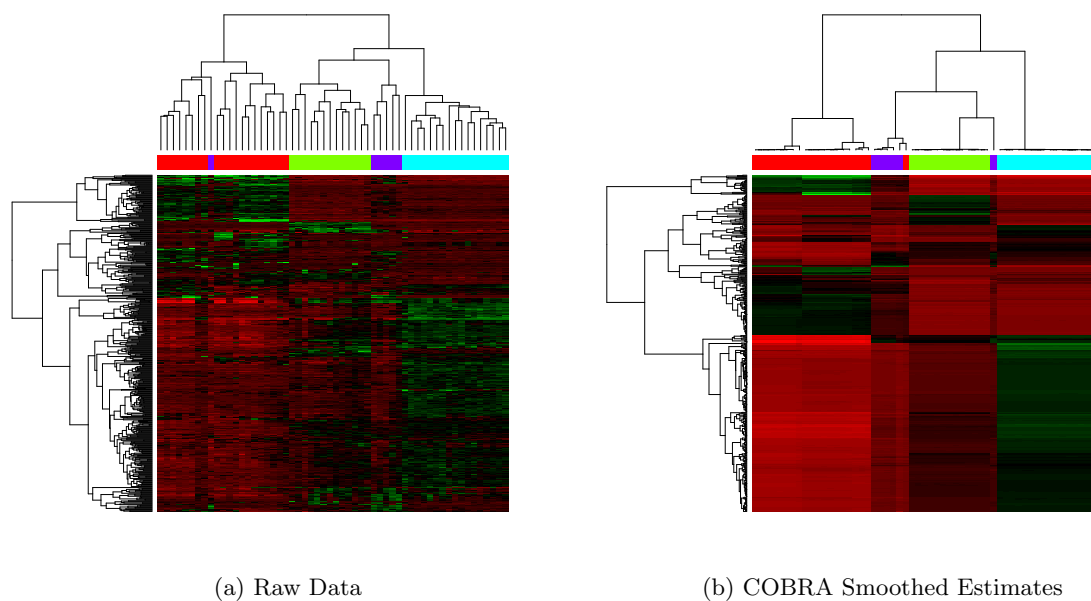


Fig 1: A heatmap of the expression of 500 genes (rows) across 56 subjects (columns) after applying hierarchical clustering on genes and subjects. [Figure 1a](#) depicts the clustered dendrogram applied to the raw data; [Figure 1b](#) depicts the results of hierarchical clustering applied to the rows and columns of COBRA smoothed estimates. Subjects belong to one of four subgroups: Normal (green), Carcinoid (red), Colon (blue), and Small Cell (purple). The color within the array indicates level of expression. Green indicates a high level of expression; red a low level of expression.

scientists have searched for molecular subtypes in other cancers, such as ovarian cancer ([Tothill et al., 2008](#)). Unfortunately, the findings in many of these additional studies have not been as reproducible as those identified by [Sørli et al. \(2001\)](#). The failure to reproduce these other results may reflect a genuine absence of biologically meaningful groupings. But another possibility may be related to issues inherent in the computational methods currently used to identify biclusters.

While numerous methods for biclustering genomic data have been proposed ([Madeira and Oliveira, 2004](#); [Busygin, Prokopyev and Pardalos, 2008](#)), the most popular approach to biclustering cancer genomics data is the clustered dendrogram. This method performs hierarchical clustering ([Hastie, Tibshirani and Friedman, 2009](#)) on the patients (columns) as well as on the genes (rows). The matrix is then re-ordered according to these separate row and column dendrograms and visualized as a heatmap with dendrograms plotted alongside the row and column axes. [Figure 1a](#) illustrates an example of a clustered dendrogram of expression data from a lung cancer study. The data consists of the expression levels of 500 genes across 56 individuals, a subset of the data studied in [Liu et al. \(2008\)](#) and [Lee et al. \(2010\)](#). Subjects belong to one of four subgroups: Normal, Carcinoid, Colon, or Small Cell. This simple strategy seems to reasonably recover the clinical diagnoses and identify sets of genes whose dysregularization characterizes the subtypes.

As an algorithmic procedure, however, the clustered dendrogram has two characteristics that make it less than ideal for generating reproducible results. Dendrograms are

constructed by greedily fusing observations (features) to decrease some criterion. Consequently the algorithm may return a biclustering that is only locally optimal with respect to the criterion. Since solutions may vary depending on how the algorithm is initialized, such procedures tend to be run from multiple initializations, but even then there is no guarantee that a global optimum will be reached. The algorithm is also not stable in the sense that small perturbations in the data can lead to large changes in the clustering assignments.

More sophisticated methods have been proposed for biclustering, some based on the singular value decomposition (SVD) of the data matrix (Lazzeroni and Owen, 2002; Bergmann, Ihmels and Barkai, 2003; Turner, Bailey and Krzanowski, 2005; Witten, Tibshirani and Hastie, 2009; Lee et al., 2010; Sill et al., 2011), and others based on graph cuts (Dhillon, 2001; Kluger et al., 2003). Some approaches are similar in spirit to the clustered dendrogram and directly cluster the rows and columns (Coifman and Gavish, 2011; Tan and Witten, 2013). While these methods may provide worthwhile improvements in empirical performance, none of them address the two fundamental issues that dog the clustered dendrogram. Moreover, scientists may shy from using many of these methods, since their outputs are typically not as easy to visualize as compared to the simple clustered dendrogram. From a reproducible research perspective, a biclustering method should (i) give the same, ideally unique, answer regardless of how the algorithm is initialized, and (ii) be stable with respect perturbations in the data.

In this paper, we pose biclustering as a convex optimization problem and introduce a novel Convex BiclusterRing Algorithm (COBRA) for iteratively solving it. COBRA outputs results that retain the simple interpretability and visualization of the clustered dendrogram and also possesses several key advantages over existing techniques: (i) **Stability and Uniqueness:** COBRA produces the unique global minimizer to a convex program and this minimizer is continuous in the data. This means that COBRA always maps the data to a single biclustering assignment, and this solution is stable. (ii) **Simplicity:** COBRA employs a single tuning parameter that controls the number of biclusters. (iii) **Data Adaptivity:** COBRA admits a simple and principled data adaptive procedure for choosing the tuning parameter that involves solving a convex matrix completion problem.

Returning to our motivating lung cancer example, Figure 1b illustrates the results of COBRA with the tuning parameter selected according to our data adaptive procedure. The columns and rows have been reordered via hierarchical clustering. Much clearer biclustering patterns emerge. Specifically, we see three distinct groups of genes and five major groups of subjects that align with the clinical diagnoses. The Carcinoid group has been partitioned into two groups that are very similar.

2. A Convex Formulation of Biclustering. Our goal is to identify the groups of rows and groups of columns in a data matrix that are associated with each other. As seen in Figure 1b, when rows and columns are reordered according to their groupings, a checkerboard pattern emerges, namely the elements of the matrix partitions defined by row and column groups tend to display a uniform intensity.

We now describe a probabilistic model that can generate the observed checkerboard pattern. Our data, $\mathbf{X} \in \mathbb{R}^{p \times n}$, consists of n samples drawn from a p -dimensional feature space. Suppose that the latent checkerboard structure is defined by R feature groups and C observation groups. If the ij th entry in \mathbf{X} belongs to the cluster defined by the r th feature group and c th observation group, then we assume that the observed value x_{ij} is given by $x_{ij} = \mu_0 + \mu_{rc} + \varepsilon_{ij}$, where μ_0 is a baseline or grand mean shared by all entries of the data matrix, μ_{rc} is the mean of the cluster defined by the r th row partition and

cth column partition, and ε_{ij} are iid $N(0, \sigma^2)$ for some $\sigma^2 > 0$. To ensure identifiability of the mean parameters, we assume that $\mu_0 = 0$, which can be achieved by removing the grand sample mean from the data matrix \mathbf{X} .

This biclustering model corresponds to a checkerboard mean model (Madeira and Oliveira, 2004). This model is most similar to that assumed by Tan and Witten (2013) who propose methods to estimate a checkerboard-like structure with some of the bicluster mean entries being sparse. The checkerboard model is exhaustive in that each matrix element is assigned to one bicluster. This is in contrast to other biclustering models that identify potentially overlapping row and column subsets that are not exhaustive; these are typically estimated using SVD-like methods (Lazzeroni and Owen, 2002; Bergmann, Ihmels and Barkai, 2003; Turner, Bailey and Krzanowski, 2005; Witten, Tibshirani and Hastie, 2009; Lee et al., 2010; Sill et al., 2011) or methods to find hot-spots (Shabalin et al., 2009).

Estimating the checkerboard model parameters consists of finding the partitions and the mean values of each partition. Estimating μ_{rc} , given feature and observation clusterings, is trivial. Let \mathcal{R} and \mathcal{C} denote the indices of the r th row partition and c th column partition. The maximum likelihood estimate of μ_{rc} is simply the sample mean of the entries of \mathbf{X} over the indices defined by \mathcal{R} and \mathcal{C} , namely $\mu_{rc} = \frac{1}{|\mathcal{R}||\mathcal{C}|} \sum_{i \in \mathcal{R}, j \in \mathcal{C}} x_{ij}$.

In contrast, estimating the row and column partitions, is a combinatorially hard problem and characterizes the main objective of biclustering. This task is akin to best subset selection in regression problems (Hastie, Tibshirani and Friedman, 2009). However, just as the best subset selection problem has been successfully attacked by solving a convex surrogate problem, namely the Lasso (Tibshirani, 1996), we will develop a convex relaxation of the combinatorially hard problem of selecting the row and column partitions.

We propose to identify the partitions by minimizing the following convex criterion

$$(2.1) \quad F_\gamma(\mathbf{U}) = \frac{1}{2} \|\mathbf{X} - \mathbf{U}\|_{\text{F}}^2 + \gamma \underbrace{\left[\Omega_{\mathbf{W}}(\mathbf{U}) + \Omega_{\tilde{\mathbf{W}}}(\mathbf{U}^{\text{T}}) \right]}_{J(\mathbf{U})},$$

where $\Omega_{\mathbf{W}}(\mathbf{U}) = \sum_{i < j} w_{ij} \|\mathbf{U}_{\cdot i} - \mathbf{U}_{\cdot j}\|_2$, and $\mathbf{U}_{\cdot i}$ ($\mathbf{U}_{\cdot i}$) denotes the i th column (row) of the matrix \mathbf{U} .

We have posed the biclustering problem as a penalized regression problem, where the matrix $\mathbf{U} \in \mathbb{R}^{p \times n}$ is our estimate of the means matrix $\boldsymbol{\mu}$. The quadratic term quantifies how well \mathbf{U} approximates \mathbf{X} . The regularization term $J(\mathbf{U})$ penalizes deviations away from a checkerboard pattern. The parameter $\gamma \geq 0$ tunes the tradeoff between the two terms. The parameters $w_{ij} = w_{ji}$ and $\tilde{w}_{ij} = \tilde{w}_{ji}$ are non-negative weights that will be explained shortly.

The penalty term $J(\mathbf{U})$ is closely related to other sparsity inducing penalties. When only the rows or columns are being clustered, minimizing the objective function in (2.1) corresponds to solving a convex clustering problem (Pelckmans et al., 2005; Lindsten, Ohlsson and Ljung, 2011; Hocking et al., 2011; Chi and Lange, 2014) under an ℓ_2 -norm fusion penalty. The convex clustering problem in turn can be seen as a generalization of the Fused Lasso (Tibshirani et al., 2005). When the ℓ_1 -norm is used in place of the ℓ_2 -norm in $\Omega_{\mathbf{W}}(\mathbf{U})$, we recover a special case of the general Fused Lasso (Tibshirani and Taylor, 2011). Other norms can also be employed in our framework; see for example Chi and Lange (2014). In this paper, we restrict ourselves to the ℓ_2 -norm since it is rotationally invariant. In general, we do not want a procedure whose biclustering output may non-trivially change when the coordinate representation of the data is trivially changed.

To understand how the regularization term $J(\mathbf{U})$ steers solutions toward a checkerboard pattern, consider the effects of $\Omega_{\mathbf{W}}(\mathbf{U})$ and $\Omega_{\tilde{\mathbf{W}}}(\mathbf{U}^\top)$ separately. Suppose $J(\mathbf{U}) = \Omega_{\mathbf{W}}(\mathbf{U})$. The i th column $\mathbf{U}_{\cdot i}$ of the matrix \mathbf{U} can be viewed as a cluster center or centroid attached to the i th column $\mathbf{X}_{\cdot i}$ of the data matrix \mathbf{X} . When $\gamma = 0$, the minimum is attained when $\mathbf{U}_{\cdot i} = \mathbf{X}_{\cdot i}$, and each column occupies a unique column cluster. As γ increases, the cluster centroids are shrunk together and in fact begin to coalesce. Two columns $\mathbf{X}_{\cdot i}$ and $\mathbf{X}_{\cdot j}$ are assigned to the same column partition if $\mathbf{U}_{\cdot i} = \mathbf{U}_{\cdot j}$. We will prove later that for sufficiently large γ , all columns coalesce into a single cluster. Similarly, suppose $J(\mathbf{U}) = \Omega_{\tilde{\mathbf{W}}}(\mathbf{U}^\top)$ and view the rows of \mathbf{U} as the cluster centroids attached to the rows of \mathbf{X} . As γ increases, the row centroids will begin to coalesce, and we likewise say that the i th and j th rows of \mathbf{X} belong to the same row partition if their centroid estimates $\mathbf{U}_{i \cdot}$ and $\mathbf{U}_{j \cdot}$ coincide.

When $J(\mathbf{U})$ includes both $\Omega_{\mathbf{W}}(\mathbf{U})$ and $\Omega_{\tilde{\mathbf{W}}}(\mathbf{U}^\top)$, rows and columns of \mathbf{U} are *simultaneously* shrunk towards each other as the parameter γ increases. The penalized estimates exhibit the desired checkerboard structure as seen in [Figure 1b](#). Note this shrinkage procedure is fundamentally different from methods like the clustered dendrogram, which independently cluster the rows and columns. By coupling row and column clustering, our formulation explicitly seeks out a solution with a checkerboard mean structure.

We now address choosing the weights w_{ij} and \tilde{w}_{ij} . A judicious choice of the weights enables us to (i) employ a single regularization parameter γ , (ii) obtain more parsimonious clusterings, and (iii) speed up the convergence of key subroutines employed by COBRA. With these goals in mind, we recommend weights having following properties: (i) The column weights should sum to $1/\sqrt{n}$ and the row weights should sum to $1/\sqrt{p}$. (ii) The column weight w_{ij} should be inversely proportional to the distance between the i th and j th columns $\|\mathbf{X}_{\cdot i} - \mathbf{X}_{\cdot j}\|_2$. The row weights should be assigned analogously. (iii) The weights should be sparse, namely consist mostly of zeros.

We now discuss the rationale behind our weight recommendations. The key to ensuring that a single tuning parameter suffices for identifying the checkerboard pattern, is keeping the two penalty terms $\Omega_{\mathbf{W}}(\mathbf{U})$ and $\Omega_{\tilde{\mathbf{W}}}(\mathbf{U}^\top)$ on the same scale. If this does not hold, then either column or row clusterings will dominate. Consequently, since the columns are in \mathbb{R}^p and the rows are in \mathbb{R}^n , we choose the column weights to sum to $1/\sqrt{p}$ and the row weights to sum to $1/\sqrt{n}$. Using weights that are inversely proportional to the distances between points, more aggressively shrinks rows and columns that are more similar to each other, and less aggressively shrinks rows and columns that are less similar to each other. Finally, sparse weights expedite computation. COBRA solves a sequence of convex clustering problems. The algorithm we employ for solving the convex clustering subproblem scales in storage and computational operations as $\mathcal{O}(npq)$, where q is the number of non-zero weights. Shrinking all pairs of columns (rows) and taking $q = n^2$ ($q = p^2$) not only increases computational costs but also typically produces inferior clustering to sparser ones as seen in [Chi and Lange \(2014\)](#). We employ the sparse Gaussian kernel weights described in [Chi and Lange \(2014\)](#), which satisfy the properties outlined above. Additional discussion on this choice of weights is given in [Appendix A](#).

3. Properties of the Convex Formulation and COBRA’s Solution. The solution to minimizing [\(2.1\)](#) has several attractive properties as a function of the data \mathbf{X} , the regularization parameter γ , and its weights $\mathbf{W} = \{w_{ij}\}$ and $\tilde{\mathbf{W}} = \{\tilde{w}_{ij}\}$, some of which can be exploited to expedite its numerical computation. We emphasize that these results are inherent to the minimization of the objective function [\(2.1\)](#). They hold regardless of the algorithm used to find the minimum point, since they are a consequence of casting the biclustering problem as a convex program. Proofs of all propositions can

be found in [Appendix B](#). First, minimizing (2.1) is a well-posed optimization problem.

PROPOSITION 3.1. *The function $F_\gamma(\mathbf{U})$ defined in (2.1) has a unique global minimizer.*

Furthermore, since $F_\gamma(\mathbf{U})$ is convex, the only local minimum is the global minimum, and any algorithm that converges to a stationary point of $F_\gamma(\mathbf{U})$ will converge to the global minimizer. The next result will have consequences for numerical computation and is also the foundation underpinning COBRA's stability.

PROPOSITION 3.2. *The minimizer \mathbf{U}^* of (2.1) is jointly continuous in $(\mathbf{X}, \gamma, \mathbf{W}, \tilde{\mathbf{W}})$.*

Continuity of \mathbf{U}^* in the regularization parameter γ suggests employing warm-starts, or using the solution at one γ as the starting point for a problem with a slightly larger γ , because small changes in γ will result in small changes in \mathbf{U}^* . Continuity of \mathbf{U}^* in \mathbf{X} tells us that the solution varies smoothly with perturbations in the data, our main stability result. Recall that the i th and j th columns (rows) are assigned to the same cluster if $\mathbf{U}_{\cdot i}^* = \mathbf{U}_{\cdot j}^*$ ($\mathbf{U}_{i \cdot}^* = \mathbf{U}_{j \cdot}^*$). Since \mathbf{U}^* varies smoothly in the data, so do the differences $\mathbf{U}_{\cdot i}^* - \mathbf{U}_{\cdot j}^*$. While assigning entries to biclusters is an inherently discrete operation, we will see in [Section 7](#) that this continuity result manifests itself in assignments that are robust to perturbations in the data. Continuity of \mathbf{U}^* in the weights also give us stability guarantees and assurances that COBRA's biclustering results should be locally insensitive to changes in the weights.

The parameter γ tunes the complexity of COBRA's solution. We next show that COBRA's most complicated (small γ) and simplest (large γ) solutions coincide with the clustered dendrogram's most complicated and simplest solutions. Clearly when $\gamma = 0$, the solution is just the data, namely $\mathbf{U}^* = \mathbf{X}$. To get some intuition on how the solution behaves as γ increases, observe that the penalty $J(\mathbf{U})$ is a semi-norm. Moreover, under suitable conditions on the weights, spelled out in [Assumption 3.1](#) below, $J(\mathbf{U})$ is zero if and only if \mathbf{U} is a constant matrix.

ASSUMPTION 3.1. *For any pair of columns (rows), indexed by i and j with $i < j$, there exists a sequence of indices $i \rightarrow k \rightarrow \dots \rightarrow l \rightarrow j$ along which the weights, w_{ik}, \dots, w_{lj} ($\tilde{w}_{ik}, \dots, \tilde{w}_{lj}$) are positive.*

PROPOSITION 3.3. *Under [Assumption 3.1](#), $J(\mathbf{U}) = 0$ if and only if $\mathbf{U} = c\mathbf{1}\mathbf{1}^\top$ for some $c \in \mathbb{R}$.*

This result suggests that as γ increases the solution to the biclustering problem converges to the solution of the following constrained optimization problem:

$$\min_{\mathbf{U}} \frac{1}{2} \|\mathbf{X} - \mathbf{U}\|_{\mathbb{F}}^2 \quad \text{subject to } \mathbf{U} = c\mathbf{1}\mathbf{1}^\top \text{ for some } c \in \mathbb{R},$$

the solution to which is just the global mean $\bar{\mathbf{X}}$, whose entries are all identically the average value of \mathbf{X} over all its entries. The next result formalizes our intuition that the centroids eventually coalesce to $\bar{\mathbf{X}}$ as γ becomes sufficiently large.

PROPOSITION 3.4. *Under [Assumption 3.1](#), $F_\gamma(\mathbf{U})$ is minimized by the grand mean $\bar{\mathbf{X}}$ for γ sufficiently large.*

Thus, as γ increases from 0, the centroids matrix \mathbf{U}^* traces a continuous solution path that starts from np biclusters, consisting of $u_{ij} = x_{ij}$, to a single bicluster, where $u_{ij} = (1/np) \sum_{i'j'} x_{i'j'}$ for all i, j .

4. Estimation of Biclusters with COBRA. Having characterized our estimator of the checkerboard means as the minimizer to (2.1), we now turn to the task of computing it. From here on, we fix the data \mathbf{X} and the weights \mathbf{W} and $\tilde{\mathbf{W}}$ and consider the biclustering solution as a function of the parameter γ , denoting the solution as \mathbf{U}_γ . The penalty term $J(\mathbf{U})$ in (2.1) makes minimization challenging since it is non-smooth and not separable over any block partitioning of \mathbf{U} . Coordinate descent (Friedman et al., 2007; Wu and Lange, 2008) is an effective solution when the non-smooth penalty term is separable over some block partitioning of the variables, which is unfortunately not the case for (2.1). Another popular iterative method for minimizing non-smooth convex functions is the alternating direction method of multipliers (ADMM) (Boyd et al., 2011). While an ADMM algorithm is feasible, we take a more direct approach with the Dykstra-like proximal algorithm (DLPA) proposed by Bauschke and Combettes (2008) because it yields a simple meta-algorithm that can take advantage of fast solvers for the convex clustering problem.

DLPA generalizes a classic algorithm for fitting restricted least squares regression problems (Dykstra, 1983) and solves minimization problems of the form

$$(4.1) \quad \min_{\mathbf{U}} \frac{1}{2} \|\mathbf{X} - \mathbf{U}\|_F^2 + f(\mathbf{U}) + g(\mathbf{U}),$$

where f and g are lower-semicontinuous, convex functions. The biclustering problem is clearly an instance of (C.1). Setting $f = \gamma\Omega_{\mathbf{W}}$ and $g = \gamma\Omega_{\tilde{\mathbf{W}}}$ in (C.1) gives us the pseudocode for COBRA shown in Algorithm 1. The operation $\text{prox}_{\gamma\Omega_{\mathbf{W}}}(\mathbf{Z})$ is the proximal mapping of the function $\gamma\Omega_{\mathbf{W}}$ and is defined to be

$$\text{prox}_{\gamma\Omega_{\mathbf{W}}}(\mathbf{Z}) = \arg \min_{\mathbf{V}} \left[\frac{1}{2} \|\mathbf{Z} - \mathbf{V}\|_2^2 + \gamma\Omega_{\mathbf{W}}(\mathbf{V}) \right].$$

Each proximal mapping in Algorithm 1 corresponds to solving a convex clustering problem.

The COBRA is very intuitive. The matrices \mathbf{Y}_m^T and \mathbf{U}_m are estimates of the means matrix at the m th iteration. The matrices \mathbf{P}_m and \mathbf{Q}_m encode discrepancies between these two estimates. We alternate between clustering the rows of the matrix $\mathbf{U}_m + \mathbf{P}_m$ and the columns of the matrix $\mathbf{Y}_m + \mathbf{Q}_m$. The following result guarantees that \mathbf{Y}_m^T and \mathbf{U}_m converge to the desired solution.

PROPOSITION 4.1. *The COBRA iterates \mathbf{U}_m and \mathbf{Y}_m^T in Algorithm 1 converge to the unique global minimizer of the convex biclustering objective (2.1).*

Proposition 4.1 not only ensures the algorithmic convergence of Algorithm 1, but it also provides a natural stopping rule. We stop iterating once $\|\mathbf{U}_m - \mathbf{Y}_m^T\|_F$ falls below some tolerance $\tau > 0$. A proof of Proposition 4.1, as well as additional technical details and discussion on DLPA and COBRA, can be found in Appendix C.

The advantage of using DLPA is that COBRA is agnostic to the actual algorithm used to solve the proximal mapping. This is advantageous since we cannot analytically compute $\text{prox}_{\gamma\Omega_{\mathbf{W}}}(\mathbf{Z})$. In this paper we use the alternating minimization algorithm (AMA) introduced in Chi and Lange (2014) to solve the convex clustering problem. The algorithm performs projected gradient ascent on the Lagrangian dual problem. Its main advantage is that it requires computational work and storage that is linear in the size of the data matrix \mathbf{X} , when we use the sparse Gaussian kernel weights described in Appendix A. Nonetheless, the DLPA framework makes it trivial to swap in more efficient solvers that may become available in the future.

Algorithm 1 Convex BiclusterRing Algorithm (COBRA)

Set $\mathbf{U}_0 = \mathbf{X}, \mathbf{P}_0 = \mathbf{0}, \mathbf{Q} = \mathbf{0}$ for $m = 0, 1, \dots$

repeat

$\mathbf{Y}_m^\top = \text{prox}_{\gamma\Omega_{\mathbf{W}}}(\mathbf{U}_m^\top + \mathbf{P}_m^\top)$ ▷ Convex Clustering of Rows

$\mathbf{P}_{m+1} = \mathbf{U}_m + \mathbf{P}_m - \mathbf{Y}_m$

$\mathbf{U}_{m+1} = \text{prox}_{\gamma\Omega_{\mathbf{W}}}(\mathbf{Y}_m + \mathbf{Q}_m)$ ▷ Convex Clustering of Columns

$\mathbf{Q}_{m+1} = \mathbf{Y}_m + \mathbf{Q}_m - \mathbf{U}_{m+1}$

until convergence

5. Model Selection. Estimating the number of clusters or biclusters in a data set is a major challenge. With many existing biclustering methods, this is further exacerbated by the many tuning parameters that must be selected and the fact that biclustering assignments do not always change smoothly with the number of biclusters. For example, the sparse SVD method (Lee et al., 2010) requires three tuning parameters: two parameters controlling the sparsity of the left and right singular vectors of the sparse SVD and one controlling its rank. Furthermore, selecting the number of biclusters and other tuning parameters can be a major computational burden for large data sets. For example, the sparse biclustering method (Tan and Witten, 2013) uses cross-validation to select the number of row and column partitions. This can be time consuming if a large range of possible number of row and column partitions are explored.

In contrast, COBRA has one parameter γ , that controls both the number of biclusters and bicluster assignments; moreover, the number of biclusters and assignments varies smoothly with γ . Encapsulating the model complexity in a single parameter γ also suggests COBRA should be more robust and stable to modest model misspecification. We will see evidence of this in the numerical experiments later.

5.1. Hold-Out Validation. We present a simple but principled approach to selecting γ in a data-driven manner by posing the model selection problem as another convex program. We randomly select a hold-out set of elements in the data matrix and assess the quality of a model \mathbf{U}_γ on how well it predicts the hold-out set. This idea was first proposed by Wold (1978) for model selection in principal component analysis and has been used more recently to select tuning parameters for matrix completion problems (Mazumder, Hastie and Tibshirani, 2010; Chi et al., 2013). Denote these index pairs $\Theta \subset \{1, \dots, p\} \times \{1, \dots, n\}$, and let $|\Theta|$ denote the cardinality of the set Θ . We may select a relatively small fraction of the elements, say 10%, for validation, namely $|\Theta| \approx 0.1 \times np$. Denote the projection operator onto the set of indices Θ by $\mathcal{P}_\Theta(\mathbf{X})$. The ij th entry of $\mathcal{P}_\Theta(\mathbf{X})$ is x_{ij} if $(i, j) \in \Theta$ and is zero otherwise. We then solve the following convex optimization problem

$$(5.1) \quad \min_{\mathbf{U}} \tilde{F}_\gamma(\mathbf{U}) := \frac{1}{2} \|\mathcal{P}_{\Theta^c}(\mathbf{X}) - \mathcal{P}_{\Theta^c}(\mathbf{U})\|_{\text{F}}^2 + \gamma J(\mathbf{U})$$

for a sequence of $\gamma \in \mathcal{G} = \{\gamma_1 = 0, \dots, \gamma_{\max}\}$. Recall that we denote the minimizer of $\tilde{F}_\gamma(\mathbf{U})$ by \mathbf{U}_γ . We choose the γ that minimizes the prediction error over the hold-out set Θ , namely $\gamma^* = \arg \min_{\gamma \in \mathcal{G}} \|\mathcal{P}_\Theta(\mathbf{X}) - \mathcal{P}_\Theta(\mathbf{U}_\gamma)\|_{\text{F}}$.

5.2. Solving the Hold-Out Problem. The problem defined in (5.1) can be seen as a convex matrix completion problem. Algorithm 2 summarizes a simple procedure for reducing the problem of minimizing $\tilde{F}_\gamma(\mathbf{U})$ to solving a sequence of the complete biclustering problems (2.1). The solution from the previous iteration is used to fill in the missing entries in the current iteration; COBRA is then applied to the complete data matrix.

Algorithm 2 COBRA with missing data

```

1: Initialize  $\mathbf{U}^{(0)}$ .
2: repeat
3:    $\mathbf{M} \leftarrow \mathcal{P}_{\Theta^c}(\mathbf{X}) + \mathcal{P}_{\Theta}(\mathbf{U}^{(m)})$ 
4:    $\mathbf{U}^{(m+1)} \leftarrow \text{COBRA}(\mathbf{M})$ 
5: until convergence

```

This approach is identical to the soft-impute approach of Mazumder, Hastie and Tibshirani (2010) for solving the matrix completion problem using a nuclear norm penalty instead of our fusion penalty $J(\mathbf{U})$. The similarity is not a coincidence as both procedures are instances of a majorization-minimization (MM) algorithm (Lange, Hunter and Yang, 2000) which apply the same majorization on the smooth quadratic term. We defer details on this connection to Appendix D. Algorithm 2 has the following convergence guarantees for the imputation algorithm.

PROPOSITION 5.1. *The limit points of the sequence of iterates $\mathbf{U}^{(m)}$ of Algorithm 2 are solutions to (5.1).*

Thus, we have turned the model selection problem of selecting both the number of biclusters and bicluster assignments into a principled convex program with strong convergence guarantees.

6. Simulation Studies. We compare COBRA to four other widely used biclustering methods with software available in R in the following simulations and real data case study in the next section. These methods are (i) the sparse biclustering method (Tan and Witten, 2013) implemented in the package `sparseBC`, (ii) Plaid models (Lazzeroni and Owen, 2002) implemented in the package `biclust`, (iii) the sparse SVD method (Lee et al., 2010; Sill et al., 2011) implemented in the package `s4vd`, and (iv) the iterative signature algorithm (Bergmann, Ihmels and Barkai, 2003) implemented in the package `isa2`. The first method is most directly comparable to ours in that it assumes an underlying checkerboard mean structure. The three other methods are popular SVD-based approaches that seek overlapping biclusters. All parameters were selected according to methods in the R packages.

In all experiments, we use the Rand index (Rand, 1971) to compare clustering results. The Rand index maps a pair of partitions to a number between 0 and 1, where 1 indicates perfect agreement between two partitions. In experiments with an underlying checkerboard partition, we consider the partition as the set of biclusters induced by taking the cross-product of the row and column groups. For all experiments, we used a single fixed weight assignment rule (See Appendix A), therefore COBRA selects a single tuning parameter γ by validation.

In the following two studies, we simulate data from a checkerboard mean pattern. Data in the first study follows the underlying model assumed by COBRA. Data in the second study follows a model with a modest amount of misspecification. Results under more drastic model misspecification, using overlapping multiplicative bicluster means assumed by Lee et al. (2010), are presented in Appendix E.

6.1. Checkerboard Mean with Gaussian noise. We first compare COBRA and the sparse biclustering (spBC) algorithm of Tan and Witten (2013) on their abilities to recover a checkerboard pattern. This simulated example is similar to the first example in Tan and Witten (2013). We simulate a 200×200 data matrix with a checkerboard

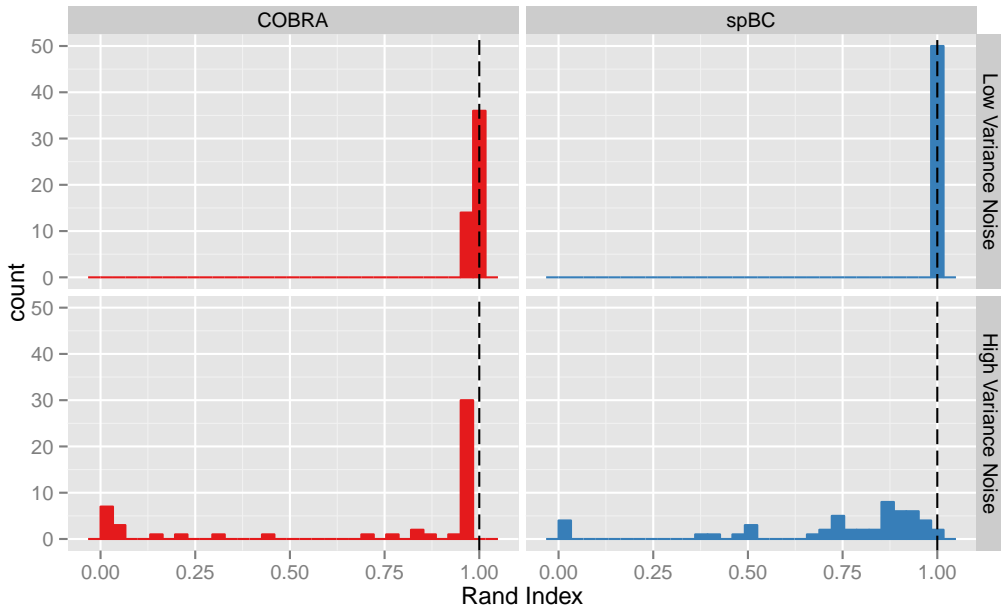


Fig 2: Checkerboard mean structure with iid $N(0, \sigma^2)$ noise: low-noise ($\sigma = 2$) and high-noise ($\sigma = 4$). Each panel shows the histogram of the Rand index of estimated and true biclusters for COBRA and spBC. In the high-noise setting, COBRA recovers the true biclusters more consistently than spBC.

bicluster structure, where $x_{ij} \sim \text{iid } N(\mu_{rc}, \sigma^2)$ and $\mu_{rc} \sim \text{Unif}[-2, 2]$. We consider a low-noise situation ($\sigma = 2$) and a high-noise one ($\sigma = 4$). There are 8 row and column groups each. Since typical clusters will not be equal in size, rows and columns are assigned to each of the groups randomly according to a non-uniform distribution. The probability that a row is assigned to the i th group is inversely proportional to i . Columns are assigned analogously to groups. We computed the Rand index between the true biclusters and those obtained by COBRA and spBC. Figure 2 shows histograms of Rand indices over 50 replicates. We see that in the low-noise setting, both methods accurately recover the biclusters defined by the row and column groups, with spBC doing slightly better. In the high-noise setting, COBRA recovers the true biclusters more consistently than spBC.

6.2. Checkerboard Mean with Outliers. Both COBRA and spBC assume additive iid Gaussian noise. We now compare how COBRA and spBC fare under a mild deviation from this assumption, namely additive heterogeneous Gaussian noise. We anticipate spBC may have trouble since it employs k -means to cluster rows and columns and k -means is known to struggle when the spread within clusters are not homogenous, as assumed in the first scenario. Consider the low-noise scenario above with the following change. Noise is bimodal; for a random 95% of the entries, the standard error is $\sigma_1 = 2$ and for the remaining 5%, the standard error σ_2 is either 5 or 10. Figure 3 shows the histograms of the Rand index of 50 replicates. We see that both methods perform well when the variance of the outlying entries is not too high. When $\sigma_2 = 10$, both methods suffer, but COBRA is noticeably more robust to outliers than spBC.

7. Application to Genomics. To illustrate COBRA in action on a real example, we revisit the lung cancer data studied by Liu et al. (2008) and Lee et al. (2010). We have selected the 500 genes with the greatest variance from the original collection of

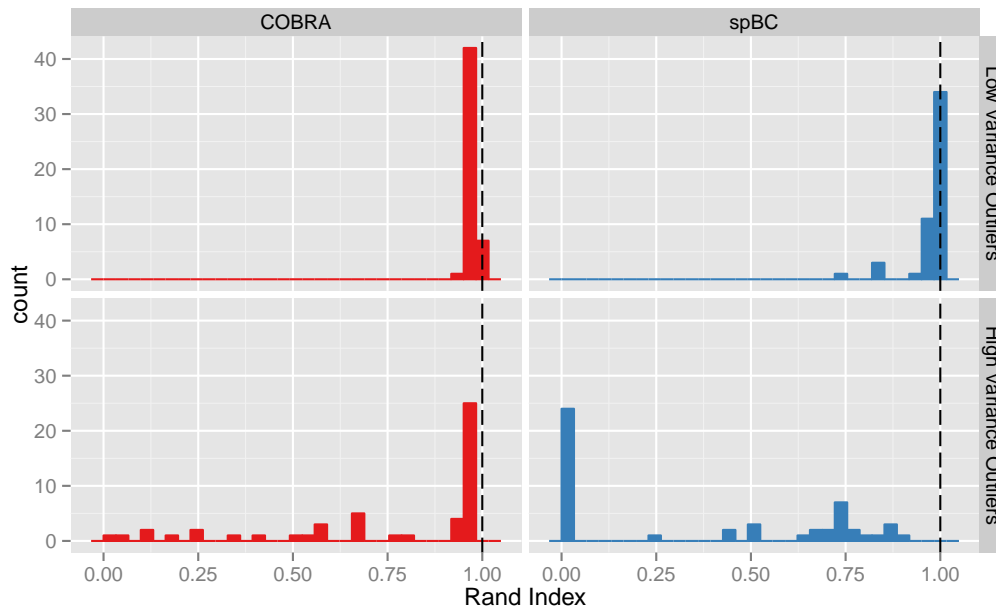


Fig 3: Checkerboard mean structure with independent two component mixture Gaussian noise. Each panel shows the histogram of the Rand index of estimated and true biclusters for COBRA and spBC. The noise in 95% of the cells is distributed as $N(0, 2^2)$, while the noise in the other 5% of the cells has either low-variance, $N(0, 5^2)$, or high-variance, $N(0, 10^2)$. When the variance is high for the outlying 5%, COBRA is noticeably more robust to outliers than spBC.

12,625 genes. Subjects belong to one of four subgroups; they are either normal subjects (Normal) or have been diagnosed with one of three types of cancers: pulmonary carcinoid tumors (Carcinoid), colon metastases (Colon), and small cell carcinoma (Small Cell).

We first illustrate how the solution \mathbf{U}_γ evolves as γ varies. Figure 4 shows snap shots of the COBRA solution path of this data set, as the parameter γ increases. The path captures the whole range of behavior between under-smoothed estimates of the mean structure (small γ), where each cell is assigned its own bicluster, to over-smoothed estimates (large γ), where all cells belong to a single bicluster. In between these extremes, we see rows and columns “fusing” together as γ increases. Thus we have visual confirmation that minimizing (2.1) over a range of γ , yields a convex formulation of the clustered dendrogram.

While generating the entire solution path enables us to visualize the hierarchical relationships between biclusterings for different γ , we may ultimately require a hard biclustering assignment. By applying the validation procedure described in Section 5, we arrive at the smoothed mean estimate shown previously in Figure 1b. The row and column orderings used in Figure 1b and Figure 4 were obtained after applying hierarchical clustering on the smoothed mean estimate. As noted earlier, we see three distinct groups of genes and five major groups of subjects which align with the ground-truth diagnoses.

We next conduct a simulation experiment based on the lung cancer data to test the stability and reproducibility of biclustering methods, critical qualities for real scientific analysis. To expedite computation in these experiments, we restrict our attention to the 200 genes with the highest variance. We first apply the five biclustering methods on the original data to obtain baseline biclusterings. We then add iid $N(0, \sigma^2)$, noise where $\sigma = 1, 2, 3$ to create a perturbed data set on which to apply the five methods. We compute the Rand index between the baseline clustering and the one obtained on the perturbed data. Figure 5 shows the histograms of the Rand index of 50 replicates. For all values of σ , we see that COBRA solutions are the most stable and reproducible.

8. Discussion. Our proposed method for biclustering, COBRA, can be considered a principled reformulation of the clustered dendrogram. Unlike the clustered dendrogram, COBRA returns a unique global minimizer of a goodness-of-fit criterion, but like the clustered dendrogram, COBRA is simple to interpret. COBRA also sports two key improvements over existing biclustering methods. First, it is more stable. COBRA biclustering assignments on perturbations of the data agree noticeably more frequently than those of existing biclustering algorithms. Second, it admits an effective and efficient model selection procedure for selecting the number of biclusters, that reduces the problem to solving a sequence of convex biclustering problems. The upshot of these two qualities is that COBRA produces results that are both simple to interpret and reproducible.

The simplicity of our means model is also its greatest weakness, since we consider only checkerboard patterns, namely we assign each observation to exactly one bicluster and do not consider overlapping biclusters (Cheng and Church, 2000; Lazzeroni and Owen, 2002; Shabalin et al., 2009). Nonetheless, while models that allow for overlapping biclusters might be more flexible, they are also harder to interpret.

While our simulation studies demonstrated the effectiveness of COBRA, there are several directions to potentially improve its performance. We could add a Lasso penalty to incentivize sparse mean estimates as in Tan and Witten (2013). While this would introduce extra complexity in choosing the regularization parameter, it may be that many genes are irrelevant and a Lasso penalty could improve biclusterings by effectively removing such genes from consideration as demonstrated in Tan and Witten (2013).

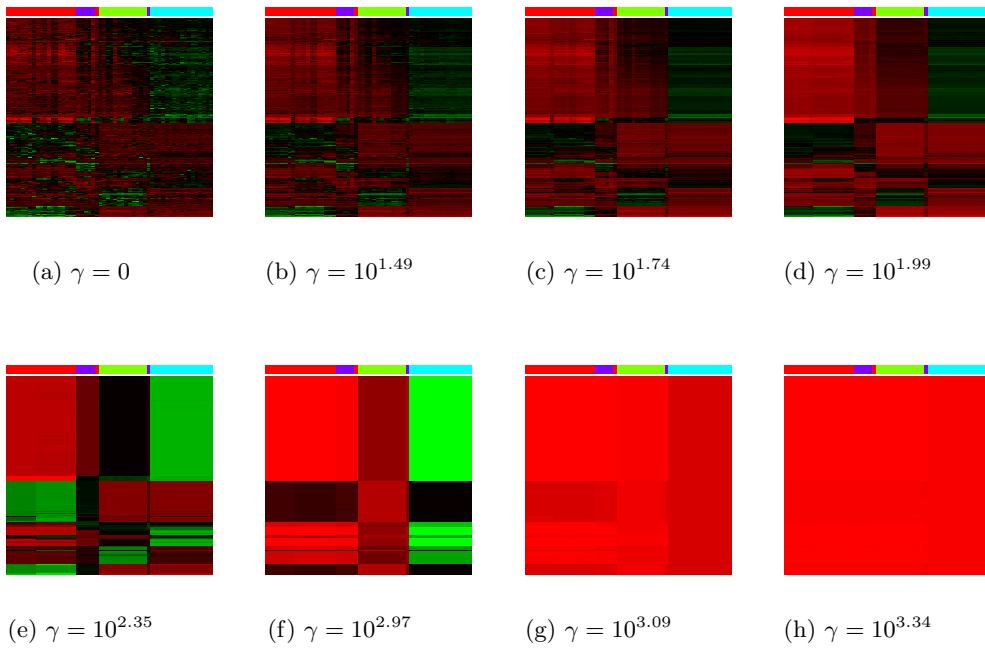


Fig 4: Snap shots of the COBRA solution path of the lung cancer data set, as the parameter γ increases. The path captures the whole range of behavior between under-smoothed estimates of the mean structure (small γ), where each cell is assigned its own bicluster, to over-smoothed estimates (large γ), where all cells belong to a single bicluster.

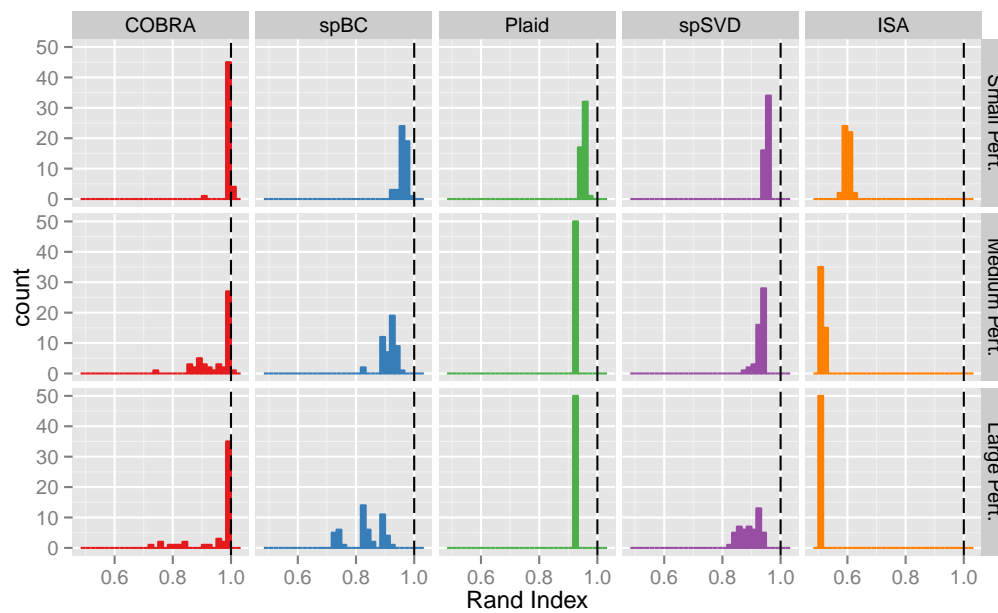


Fig 5: Stability and reproducibility of biclusterings in lung cancer microarray data. COBRA and four other biclustering methods are applied to the lung cancer data to obtain baseline biclusterings. We then perturb the data by adding iid $N(0, \sigma^2)$ noise where $\sigma = 1$ (Small Pert.), 2 (Medium Pert.), 3 (Large Pert.). Each panel shows the histogram of the Rand index between the baseline clustering and the one obtained on the perturbed data. For all values of σ , we see that COBRA solutions are the most stable and reproducible.

As with all convex shrinkage estimators, the COBRA solution is biased, and in particular biased towards the grand mean of the data matrix. We can mitigate this bias using a two stage procedure analogous to the relaxed Lasso (Meinshausen, 2007), by recomputing weights based on the smoothed output of an initial application of COBRA and then reapplying COBRA using the new weights. Alternatively, we could consider non-convex penalties (Pan, Shen and Liu, 2013) that would also produce less biased estimates. The drawback of the latter approach is that we would lose the computational guarantees of the convex formulation.

In general, the COBRA solution paths are not guaranteed to be agglomerative. In the special case of convex clustering with the ℓ_1 -norm with uniform weights $w_{ij} = 1$, Hocking et al. (2011) prove that the path is agglomerative. They also give an ℓ_2 -norm example in which the centroids fuse and then unfuse as the regularization parameter increases. This behavior, however, seems to occur infrequently in practice. Nonetheless, COBRA allows for such fission events. We conjecture that under certain conditions on the weights, we can limit the probability of these fissions; this is something we will investigate in future work.

Finally, we highlight some parallel work in the signal processing literature. Coifman and Gavish (2011) explore the biclustering problem through a novel wavelet representation of the transposable data matrix. They also seek a representation that is smooth with respect to partitions of the row and column graphs that specify the similarity among the observations and features. By casting the problem in a signal processing framework, however, a checkerboard mean structure can be obtained via operations in the wavelet domain, namely by thresholding small wavelet coefficients. We leave it as future work to determine the connections between our simple and direct formulation of the biclustering problem with Coifman and Gavish’s wavelet representation of the problem.

An R package implementing COBRA will be made available.

Acknowledgements. EC acknowledges support from CIA Postdoctoral Fellowship 2012-12062800003. GA acknowledges support from NSF DMS 1209017, 1264058, and 1317602. RB acknowledges support from ARO MURI W911NF-09-1-0383 and AFOSR grant FA9550-14-1-0088.

APPENDIX A: COLUMN AND ROW WEIGHTS

Recall that our goal is to minimize the following convex criterion

$$F_\gamma(\mathbf{U}) = \frac{1}{2} \|\mathbf{X} - \mathbf{U}\|_F^2 + \underbrace{\gamma \left[\Omega_{\mathbf{W}}(\mathbf{U}) + \Omega_{\tilde{\mathbf{W}}}(\mathbf{U}^T) \right]}_{J(\mathbf{U})},$$

where $\Omega_{\mathbf{W}}(\mathbf{U}) = \sum_{i < j} w_{ij} \|\mathbf{U}_{\cdot i} - \mathbf{U}_{\cdot j}\|_2$, and $\mathbf{U}_{\cdot i}$ ($\mathbf{U}_{i \cdot}$) denotes the i th column (row) of the matrix \mathbf{U} . In this work, we use the sparse Gaussian kernel weights proposed in Chi and Lange (2014) for the weights \mathbf{W} and $\tilde{\mathbf{W}}$ that define the terms $\Omega_{\mathbf{W}}(\mathbf{U})$ and $\Omega_{\tilde{\mathbf{W}}}(\mathbf{U})$.

We construct the weights in two steps. We describe these steps for computing the column weights; the row weights are computed analogously. We start by computing pre-weights between the i th and j th columns as $\hat{w}_{ij} = \iota_{\{i,j\}}^k \exp(-\phi \|\mathbf{X}_{\cdot i} - \mathbf{X}_{\cdot j}\|_2^2)$, as the product of two terms. The first factor $\iota_{\{i,j\}}^k$ is 1 if j is among i ’s k -nearest-neighbors or vice versa and 0 otherwise. The first term controls the sparsity of the weights. The second factor is a Gaussian kernel that puts greater pressure on similar columns to fuse and less pressure on dissimilar columns to fuse. The nonnegative constant ϕ controls the rate at which the pressure to fuse is applied as a function of the distance between

columns; the value $\phi = 0$ corresponds to uniform weights. The pre-weights \hat{w}_{ij} are then normalized to sum to $1/\sqrt{p}$.

For all experiments in the paper, we set $\phi = 0.5$ and set $k = 10$ for both row and column weights.

We briefly discuss the rationale behind our weight choice here and refer readers to [Chi and Lange \(2014\)](#) for a more detailed exposition. [Chi and Lange \(2014\)](#) give several examples that show that restricting positive weights to nearest neighbors enhances both computational efficiency and clustering quality. In their examples they showed that if dense Gaussian kernel weights were used, cluster centroids shrunk towards each other as the tuning parameter γ increased but no fusions would occur along the path save a single simultaneous fusion of all cluster centroids for a sufficiently large γ . Thus, while the two factors defining the weights act similarly, sensible fusions along the solution path could be achieved only by using them together. This is best illustrated in the half-moons example in ([Chi and Lange, 2014](#)).

APPENDIX B: PROOFS OF SOLUTION PROPERTIES

In this appendix, we give proofs of propositions in [Section 3](#) in the paper.

PROPOSITION B.1 (Existence and Uniqueness). *The function $F_\gamma(\mathbf{U})$ defined in (2.1) has a unique global minimizer.*

We first recall a few definitions and concepts useful in optimization ([Lange, 2013](#)). A function is *coercive* if all its sub level sets are compact. A function f is *convex* if $f(\alpha\mathbf{x} + (1 - \alpha)\mathbf{y}) \leq \alpha f(\mathbf{x}) + (1 - \alpha)f(\mathbf{y})$ for all $\alpha \in (0, 1)$ and \mathbf{x}, \mathbf{y} in its domain. A function f is *strictly convex* if the inequality is strict.

PROOF. The existence and uniqueness of a global minimizer \mathbf{U}^* are immediate consequences of the coerciveness and strict convexity of $F_\gamma(\mathbf{U})$. □

PROPOSITION B.2 (Continuity). *The solution \mathbf{U}^* of (2.1) is jointly continuous in $(\mathbf{X}, \gamma, \mathbf{W}, \tilde{\mathbf{W}})$.*

PROOF. Without loss of generality, we can absorb the regularization parameter γ into the weights $\mathbf{w} = (\text{vec}(\mathbf{W})^\top, \text{vec}(\tilde{\mathbf{W}})^\top)^\top \in \mathbb{R}^{\frac{p(p-1)}{2} + \frac{n(n-1)}{2}}$. Thus, we can check to see if the solution \mathbf{U}^* is continuous in the variable $\zeta = (\text{vec}(\mathbf{X})^\top, \mathbf{w}^\top)^\top$. It is easy to verify that the following function is jointly continuous in \mathbf{U} and ζ

$$f(\mathbf{U}, \zeta) = \frac{1}{2} \|\mathbf{X} - \mathbf{U}\|_F^2 + J_{\mathbf{w}}(\mathbf{U}),$$

where

$$J_{\mathbf{w}}(\mathbf{U}) = \frac{1}{\sqrt{p}} \Omega_{\mathbf{w}}(\mathbf{U}) + \frac{1}{\sqrt{n}} \Omega_{\tilde{\mathbf{w}}}(\mathbf{U}^\top)$$

is a convex function of \mathbf{U} that is continuous in \mathbf{w} . Let

$$\mathbf{U}^*(\zeta) = \arg \min_{\mathbf{U}} f(\mathbf{U}, \zeta).$$

We proceed with a proof by contradiction. Suppose $\mathbf{U}^*(\zeta)$ is not continuous at a point ζ . Then there exists an $\epsilon > 0$ and a sequence $\{\zeta^{(m)}\}$ converging to ζ such that $\|\mathbf{U}^{(m)} - \mathbf{U}^*(\zeta)\|_F \geq \epsilon$ for all m where

$$\mathbf{U}^{(m)} = \arg \min_{\mathbf{U}} f(\mathbf{U}, \zeta^{(m)}).$$

Note that since $f(\mathbf{U}, \zeta)$ is strongly convex in \mathbf{U} , the minimizers $\mathbf{U}^{(m)}$ and $\mathbf{U}^*(\zeta)$ exist and are unique. Without loss of generality we can assume $\|\zeta^{(m)} - \zeta\|_F \leq 1$. This fact will be used later in proving the boundedness of the sequence $\mathbf{U}^{(m)}$.

Fix an arbitrary point $\tilde{\mathbf{U}}$. If $\mathbf{U}^{(m)}$ is a bounded sequence then we can pass to a convergent subsequence with limit $\bar{\mathbf{U}}$. Note that $f(\mathbf{U}^{(m)}, \zeta^{(m)}) \leq f(\tilde{\mathbf{U}}, \zeta^{(m)})$ for all m . Since f is continuous in (\mathbf{U}, ζ) , taking limits gives us the inequality

$$f(\bar{\mathbf{U}}, \zeta) \leq f(\tilde{\mathbf{U}}, \zeta).$$

Since $\tilde{\mathbf{U}}$ was selected arbitrarily, it follows that $\bar{\mathbf{U}} = \mathbf{U}^*(\zeta)$, which is a contradiction. It only remains for us to show that the sequence $\mathbf{U}^{(m)}$ is bounded.

Consider the function

$$g(\mathbf{U}) = \sup_{\tilde{\zeta}: \|\tilde{\zeta} - \zeta\|_F \leq 1} \frac{1}{2} \|\tilde{\mathbf{X}} - \mathbf{U}\|_F^2 + J_{\tilde{\mathbf{w}}}(\mathbf{U}).$$

Note that g is convex, since it is the point-wise supremum of a collection of convex functions. Since $f(\mathbf{U}, \zeta^{(m)}) \leq g(\mathbf{U})$ and f is strongly convex in \mathbf{U} , it follows that $g(\mathbf{U})$ is also strongly convex and therefore has a unique global minimizer \mathbf{U}^* such that $g(\mathbf{U}^*) < \infty$. It also follows that

$$(B.1) \quad f(\mathbf{U}^{(m)}, \zeta^{(m)}) \leq f(\mathbf{U}^*, \zeta^{(m)}) \leq g(\mathbf{U}^*)$$

for all m . By the reverse triangle inequality it follows that

$$(B.2) \quad \frac{1}{2} \left(\|\mathbf{U}^{(m)}\|_F - \|\mathbf{X}^{(m)}\|_F \right)^2 \leq \frac{1}{2} \|\mathbf{U}^{(m)} - \mathbf{X}^{(m)}\|_F^2 \leq f(\mathbf{U}^{(m)}, \zeta^{(m)}).$$

Combining the inequalities in (B.1) and (B.2), we arrive at the conclusion that

$$\frac{1}{2} \left(\|\mathbf{U}^{(m)}\|_F - \|\mathbf{X}^{(m)}\|_F \right)^2 \leq g(\mathbf{U}^*),$$

for all m . Suppose the sequence $\mathbf{U}^{(m)}$ is unbounded, namely $\|\mathbf{U}^{(m)}\|_F \rightarrow \infty$. But since $\mathbf{X}^{(m)}$ converges to \mathbf{X} , the left hand side must diverge. Thus, we arrive at a contradiction if $\mathbf{U}^{(m)}$ is unbounded. □

PROPOSITION B.3 (Zeroes of the fusion penalty). *Under Assumption 3.1, $J(\mathbf{U}) = 0$ if and only if $\mathbf{U} = c\mathbf{1}\mathbf{1}^\top$ for some $c \in \mathbb{R}$.*

PROOF. We first show that

$$\Omega_{\mathbf{w}}(\mathbf{U}) = \sum_{i < j} w_{ij} \|\mathbf{U}_{\cdot i} - \mathbf{U}_{\cdot j}\|_F$$

is positive if and only if $\mathbf{U}_{\cdot i} = \mathbf{U}_{\cdot j}$ for all $i < j$, namely all the columns of \mathbf{U} are the same. Clearly if the columns of \mathbf{U} are the same, then $\Omega_{\mathbf{w}}(\mathbf{U})$ is zero. Suppose that

$\Omega_{\mathbf{W}}(\mathbf{U})$ is zero. Then it must be that $\mathbf{U}_{\cdot i} = \mathbf{U}_{\cdot j}$ for every $w_{ij} > 0$. Consider a pair (i, j) such that $w_{ij} = 0$. By [Assumption 3.1](#), there exists a path $i \rightarrow k \rightarrow \dots \rightarrow l \rightarrow j$ along which the weights are positive. Let w denote the smallest weight along this path, namely $w = \min\{w_{ik}, \dots, w_{lj}\}$. By the triangle inequality

$$\|\mathbf{U}_{\cdot i} - \mathbf{U}_{\cdot j}\|_{\text{F}} \leq \|\mathbf{U}_{\cdot i} - \mathbf{U}_{\cdot k}\|_{\text{F}} + \dots + \|\mathbf{U}_{\cdot l} - \mathbf{U}_{\cdot j}\|_{\text{F}}.$$

We can then conclude that

$$w\|\mathbf{U}_{\cdot i} - \mathbf{U}_{\cdot j}\|_{\text{F}} \leq \Omega_{\mathbf{W}}(\mathbf{U}) = 0.$$

It follows that $\mathbf{U}_{\cdot i} = \mathbf{U}_{\cdot j}$, since w is positive. By a similar argument it follows that

$$\Omega_{\tilde{\mathbf{W}}}(\mathbf{U}) = \sum_{i < j} \tilde{w}_{ij} \|\mathbf{U}_{\cdot i} - \mathbf{U}_{\cdot j}\|_{\text{F}}$$

is zero if and only if $\mathbf{U}_{\cdot i} = \mathbf{U}_{\cdot j}$ for all $i < j$, or in other words if the rows of \mathbf{U} are all the same. Thus, $J_{\mathbf{W}}(\mathbf{U}) = 0$ if and only if \mathbf{U} is a constant matrix. \square

PROPOSITION B.4 (Coalescence). *Under [Assumption 3.1](#), $F_{\gamma}(\mathbf{U})$ is minimized by the grand mean $\bar{\mathbf{X}}$ for γ sufficiently large.*

PROOF. We will show that there is a γ_{\max} such that for all $\gamma \geq \gamma_{\max}$, the grand mean matrix $\bar{\mathbf{X}}$ is the unique global minimizer to the primal objective [\(2.1\)](#). We will certify that $\bar{\mathbf{X}}$ is the solution to the primal problem by showing that the optimal value of a dual problem, which lower bounds the primal, equals $F_{\gamma}(\bar{\mathbf{X}})$.

Throughout the proof, we will work with the vectorization of matrices, namely the vector obtained by stacking the columns of a matrix on top of each other. We denote the vectorization of a matrix \mathbf{X} by its corresponding bold lower case, namely $\mathbf{x} = \text{vec}(\mathbf{X})$. Thus, we will construct a dual to the following representation of the primal problem,

$$(B.3) \quad \underset{\mathbf{u}}{\text{minimize}} \quad F_{\gamma}(\mathbf{u}) = \frac{1}{2} \|\mathbf{x} - \mathbf{u}\|_2^2 + \gamma J(\mathbf{u}).$$

In order to rewrite the penalty J in terms of the vector \mathbf{u} , we use the identity $\text{vec}(\mathbf{MNP}) = (\mathbf{P}^{\text{T}} \otimes \mathbf{M}) \text{vec}(\mathbf{N})$ where \otimes denotes the Kronecker product between two matrices. Thus,

$$J(\mathbf{u}) = \sum_{i < j} w_{ij} \|\mathbf{A}_{ij} \mathbf{u}\|_2 + \sum_{i < j} \tilde{w}_{ij} \|\tilde{\mathbf{A}}_{ij} \mathbf{u}\|_2,$$

where

$$\begin{aligned} \mathbf{A}_{ij} &= (\mathbf{e}_i - \mathbf{e}_j)^{\text{T}} \otimes \mathbf{I}, \\ \tilde{\mathbf{A}}_{ij} &= \mathbf{I} \otimes (\mathbf{e}_i - \mathbf{e}_j)^{\text{T}}, \end{aligned}$$

and \mathbf{e}_i is the i th standard basis vector. To keep things notationally simpler, we have absorbed the normalizations by \sqrt{p} and \sqrt{n} into the weights w_{ij} and \tilde{w}_{ij} .

We first introduce some notation in order to write the relevant dual problem to the primal problem [\(B.3\)](#). Note that the column weights w_{ij} can be identified with a column graph of n nodes, where there is an edge between the i th and j th node if and only if $w_{ij} > 0$. The row weights \tilde{w}_{ij} can also be identified with an analogous row graph of p nodes. Let \mathcal{E}_c and \mathcal{E}_r denote the sets of edges in the column and row graphs, and let $|\mathcal{E}_c|$

and $|\mathcal{E}_r|$ denote their respective cardinalities. The edge-incidence matrix of the column graph $\Phi_c \in \mathbb{R}^{|\mathcal{E}_c| \times n}$ encodes its connectivity and is defined as

$$\phi_{c,li} = \begin{cases} 1 & \text{If node } i \text{ is the head of edge } l, \\ -1 & \text{If node } i \text{ is the tail of edge } l, \\ 0 & \text{otherwise.} \end{cases}$$

The row edge-incidence matrix $\Phi_r \in \mathbb{R}^{|\mathcal{E}_r| \times p}$ is defined similarly.

We begin deriving the dual problem by recalling that norms possess a variational representation in terms of their dual norms, namely

$$\|\mathbf{y}\| = \max_{\|\mathbf{z}\|_{\dagger} \leq 1} \langle \mathbf{z}, \mathbf{y} \rangle,$$

where $\|\cdot\|_{\dagger}$ is the dual norm of $\|\cdot\|$. Using this fact and working through some tedious algebra, we can rewrite the penalty term in (B.3) compactly as

$$\gamma J(\mathbf{u}) = \max_{\mathbf{v} \in C_{\gamma}} \langle \mathbf{A}^{\top} \mathbf{v}, \mathbf{u} \rangle.$$

The vector \mathbf{v} is the concatenation of several vectors, namely

$$\mathbf{v} = (\mathbf{v}_1^{\top}, \dots, \mathbf{v}_{\mathcal{E}_c}^{\top}, \tilde{\mathbf{v}}_1^{\top}, \dots, \tilde{\mathbf{v}}_{\mathcal{E}_r}^{\top})^{\top},$$

where $\mathbf{v}_l \in \mathbb{R}^n$, $\tilde{\mathbf{v}}_l \in \mathbb{R}^p$. The matrix \mathbf{A} can be expressed in terms of the row and column edge-incidence matrices, namely

$$\mathbf{A} = \begin{pmatrix} \Phi_c \otimes \mathbf{I} \\ \mathbf{I} \otimes \Phi_r \end{pmatrix}.$$

Finally, the constraints on the vector \mathbf{v} are encoded in the set $C_{\gamma} = \{\mathbf{v} : \|\mathbf{v}_l\|_2 \leq w_l \gamma \text{ and } \|\tilde{\mathbf{v}}_l\|_2 \leq \tilde{w}_l \gamma\}$.

Thus, the primal problem (B.3) can be expressed as the following saddle point problem

$$(B.4) \quad \max_{\mathbf{v} \in C_{\gamma}} \min_{\mathbf{u}} \frac{1}{2} \|\mathbf{x} - \mathbf{u}\|_2^2 + \langle \mathbf{A}^{\top} \mathbf{v}, \mathbf{u} \rangle.$$

By performing the minimization with respect to \mathbf{u} , we obtain a dual maximization problem that provides a lower bound on the primal objective

$$\max_{\mathbf{v} \in C_{\gamma}} -\frac{1}{2} \|\mathbf{A}^{\top} \mathbf{v}\|_2^2 + \langle \mathbf{v}, \mathbf{A} \mathbf{x} \rangle.$$

For sufficiently large γ , the solution to the dual maximization problem coincides with the solution to the unconstrained maximization problem

$$\max_{\mathbf{v}} -\frac{1}{2} \|\mathbf{A}^{\top} \mathbf{v}\|_2^2 + \langle \mathbf{v}, \mathbf{A} \mathbf{x} \rangle,$$

whose solution is $\mathbf{v}^* = (\mathbf{A} \mathbf{A}^{\top})^{\dagger} \mathbf{A} \mathbf{x}$. Plugging \mathbf{v}^* into the dual objective gives an optimal value of

$$\frac{1}{2} \|\mathbf{A}^{\top} (\mathbf{A} \mathbf{A}^{\top})^{\dagger} \mathbf{A} \mathbf{x}\|_2^2,$$

which we rewrite as

$$\frac{1}{2} \|\mathbf{x} - \left[\mathbf{I} - \mathbf{A}^\top (\mathbf{A}\mathbf{A}^\top)^\dagger \mathbf{A} \right] \mathbf{x}\|_2^2.$$

Note that $\left[\mathbf{I} - \mathbf{A}^\top (\mathbf{A}\mathbf{A}^\top)^\dagger \mathbf{A} \right]$ is the projection onto the orthogonal complement of the column space of \mathbf{A}^\top , which is equivalent to the null space or kernel of \mathbf{A} , denoted $\text{Ker}(\mathbf{A})$. We will show shortly that $\text{Ker}(\mathbf{A})$ is the span of the all ones vector. Therefore, $\left[\mathbf{I} - \mathbf{A}^\top (\mathbf{A}\mathbf{A}^\top)^\dagger \mathbf{A} \right] \mathbf{x} = \frac{1}{np} \langle \mathbf{x}, \mathbf{1} \rangle \mathbf{1}$.

Before showing that $\text{Ker}(\mathbf{A})$ is the span of $\mathbf{1}$, we note that the smallest γ such that $\mathbf{v}^* \in C_\gamma$ is an upper bound on γ_{\max} .

We now argue that $\text{Ker}(\mathbf{A})$ is the span of $\mathbf{1} \in \mathbb{R}^{np}$. We rely on the following fact: If Φ is an incidence matrix of a connected graph with n vertices, then the rank of Φ is $n - 1$ (See Theorem 7.2 in Chapter 7 of [Deo \(1974\)](#)). According to [Assumption 3.1](#) in the paper, the column and row graphs are connected; it follows that $\Phi_c \in \{-1, 0, 1\}^{|\mathcal{E}_c| \times n}$ has rank $n - 1$ and $\Phi_r \in \{-1, 0, 1\}^{|\mathcal{E}_r| \times p}$ has rank $p - 1$. It follows then that $\text{Ker}(\Phi_c)$ and $\text{Ker}(\Phi_r)$ have dimension one. Furthermore, since each row of Φ_c and Φ_r has one 1 and one -1 , it follows that $\mathbf{1} \in \text{Ker}(\Phi_c) \subset \mathbb{R}^n$, and likewise $\mathbf{1} \in \text{Ker}(\Phi_r) \subset \mathbb{R}^p$. A vector $\mathbf{z} \in \text{Ker}(\mathbf{A})$ if and only if $\mathbf{z} \in \text{Ker}(\Phi_c \otimes \mathbf{I}) \cap \text{Ker}(\mathbf{I} \otimes \Phi_r)$.

Recall that if the singular values of a matrix \mathbf{A} are $\sigma_{\mathbf{A},i}$ and the singular values of a matrix \mathbf{B} are $\sigma_{\mathbf{B},j}$, then the singular values of their Kronecker product $\mathbf{A} \otimes \mathbf{B}$ are $\sigma_{\mathbf{A},i} \sigma_{\mathbf{B},j}$. It follows then that the rank of $\mathbf{A} \otimes \mathbf{B}$ is the product of the ranks of \mathbf{A} and \mathbf{B} .

The above rank property of Kronecker products of matrices implies that the dimension of $\text{Ker}(\Phi_c \otimes \mathbf{I})$ equals p and the dimension of $\text{Ker}(\mathbf{I} \otimes \Phi_r)$ equals n . It is easy to see then that the linearly independent set of vectors $\{\mathbf{1} \otimes \mathbf{e}_1, \dots, \mathbf{1} \otimes \mathbf{e}_p\}$, where $\mathbf{1} \in \mathbb{R}^n$ and $\mathbf{e}_i \in \mathbb{R}^p$, forms a basis for $\text{Ker}(\Phi_c \otimes \mathbf{I})$. Likewise, the linearly independent set of vectors $\{\mathbf{e}_1 \otimes \mathbf{1}, \dots, \mathbf{e}_n \otimes \mathbf{1}\}$, where $\mathbf{1} \in \mathbb{R}^p$ and $\mathbf{e}_i \in \mathbb{R}^n$, forms a basis for $\text{Ker}(\mathbf{I} \otimes \Phi_r)$.

Take an element from $\text{Ker}(\Phi_c \otimes \mathbf{I})$, namely $\mathbf{1} \otimes \mathbf{a}$, where $\mathbf{1} \in \mathbb{R}^n$ and $\mathbf{a} \in \mathbb{R}^p$. We will show that in order for $\mathbf{1} \otimes \mathbf{a} \in \text{Ker}(\mathbf{I} \otimes \Phi_r)$, \mathbf{a} must be a multiple of $\mathbf{1}$. Consider the relevant matrix-vector product

$$(\mathbf{I} \otimes \Phi_r)(\mathbf{1} \otimes \mathbf{a}) = (\mathbf{I} \otimes \Phi_r) \text{vec}(\mathbf{a}\mathbf{1}^\top) = \Phi_r \mathbf{a}\mathbf{1}^\top,$$

where we again used the fact that $\text{vec}(\mathbf{M}\mathbf{N}\mathbf{P}) = (\mathbf{P}^\top \otimes \mathbf{M}) \text{vec}(\mathbf{N})$ and the fact that $\text{vec}(\mathbf{b}\mathbf{c}^\top) = \mathbf{c} \otimes \mathbf{b}$. Note that $(\mathbf{I} \otimes \Phi_r)(\mathbf{1} \otimes \mathbf{a}) = \mathbf{0}$ if and only if $\Phi_r \mathbf{a} = \mathbf{0}$. But the only way for $\Phi_r \mathbf{a}$ to be zero is for $\mathbf{a} = c\mathbf{1}$ for some $c \in \mathbb{R}$. A similar argument shows that the only non-trivial vector in $\text{Ker}(\mathbf{I} \otimes \Phi_r)$ that also belongs to $\text{Ker}(\Phi_c \otimes \mathbf{I})$ is $\tilde{c}\mathbf{1}$ for $\tilde{c} \in \mathbb{R}$. Thus, we have shown that $\text{Ker}(\mathbf{A})$ is the span of $\mathbf{1}$. \square

APPENDIX C: DLPA, COBRA, AND A PROOF OF PROPOSITION 4.1

We give expanded technical treatment of DLPA and COBRA as well as results described in Section 4. We begin by reviewing some basic concepts convex analysis ([Bauschke and Combettes, 2008](#); [Combettes and Pesquet, 2011](#)). Recall that the domain of a convex function f is the set of \mathbf{x} such that $f(\mathbf{x}) < \infty$. For $\sigma > 0$ the mapping

$$\text{prox}_{\sigma f}(\mathbf{u}) = \arg \min_{\mathbf{v}} \left[\sigma f(\mathbf{v}) + \frac{1}{2} \|\mathbf{u} - \mathbf{v}\|_2^2 \right]$$

is called the proximal map of the function $f(\mathbf{v})$. The proximal map exists and is unique whenever the function $f(\mathbf{v})$ is convex and lower-semicontinuous. Norms and semi-norms

satisfy these conditions, and for many norms of interest the proximal map can be evaluated by either an explicit formula or an efficient algorithm. For example, the proximal map for the ℓ_1 -norm is the ubiquitous element-wise soft-thresholding operator, namely the l th element of the proximal mapping is given by

$$\left[\text{prox}_{\sigma\|\cdot\|_1}(\mathbf{u})\right]_l = \left[1 - \frac{\sigma}{|u_l|}\right]_+ u_l.$$

Closer inspection of (2.1) shows that we seek the proximal mapping of the sum of two lower-semicontinuous, convex functions, namely

$$\text{prox}_{f+g}(\mathbf{U}) = \arg \min_{\mathbf{U}} \frac{1}{2}\|\mathbf{X} - \mathbf{U}\|_{\text{F}}^2 + f(\mathbf{U}) + g(\mathbf{U}),$$

where $f(\mathbf{U}) = \gamma\Omega_{\mathbf{W}}(\mathbf{U})$ and $g(\mathbf{U}) = \gamma\Omega_{\tilde{\mathbf{W}}}(\mathbf{U}^{\text{T}})$.

This problem is reminiscent of the classic problem of finding the projection of a point onto the intersection of two nonempty and closed convex sets. Indeed, it is the problem when the functions f and g are respectively the indicator functions of two nonempty and closed convex sets A and B . Then we can pose the problem of finding the projection of \mathbf{X} onto the set $A \cap B$ as the optimization problem

$$\min_{\mathbf{U}} \frac{1}{2}\|\mathbf{X} - \mathbf{U}\|_{\text{F}}^2 + \delta_A(\mathbf{U}) + \delta_B(\mathbf{U}),$$

where δ_A is the set indicator function, which is 0 for all $\mathbf{U} \in A$ and ∞ for all $\mathbf{U} \notin A$.

von Neumann's alternating projection method provides an iterative solution when the two sets A and B are vector subspaces (Deutsch, 1992). His strategy was subsequently generalized by Dykstra to closed convex cones in Euclidean spaces (Dykstra, 1983) and generalized further by Boyle and Dykstra to the intersection of convex sets in Hilbert spaces (Boyle and Dykstra, 1986). Finally, Bauschke and Combettes (2008) derived a Dykstra-like proximal algorithm that iteratively solves for the desired proximal mapping of the sum of two convex functions (Bauschke and Combettes, 2008; Combettes and Pesquet, 2011), which we describe next.

Let f and g be lower-semicontinuous convex functions on \mathbb{R}^n , with $\text{dom } f \cap \text{dom } g \neq \emptyset$, and let $\mathbf{x} \in \mathbb{R}^n$. Bauschke and Combettes' algorithm, shown in Algorithm 3, iteratively solves the following problem

$$(C.1) \quad \min_{\mathbf{u} \in \mathbb{R}^n} \frac{1}{2}\|\mathbf{u} - \mathbf{x}\|_2^2 + f(\mathbf{u}) + g(\mathbf{u})$$

and is guaranteed to converge.

THEOREM C.1 (Proposition 5.3 in Combettes and Pesquet (2011)). *Algorithm 3 converges to the solution of (C.1).*

Setting $f(\mathbf{U}) = \gamma\Omega_{\mathbf{W}}(\mathbf{U})$ and $g(\mathbf{U}) = \gamma\Omega_{\tilde{\mathbf{W}}}(\mathbf{U})$ in Algorithm 3 yields COBRA outlined in Algorithm 1 in the paper. Consequently, the convergence of COBRA (Proposition 4.1) follows immediately from Theorem C.1, since $\Omega_{\mathbf{W}}(\mathbf{U})$ and $\Omega_{\tilde{\mathbf{W}}}(\mathbf{U})$ are both continuous convex functions over all of \mathbb{R}^{np} .

Algorithm 3 Dykstra-Like Proximal Algorithm (DLPA)Set $\mathbf{u}_0 = \mathbf{x}, \mathbf{p}_0 = \mathbf{0}, \mathbf{q} = \mathbf{0}$ for $m = 0, 1, \dots$ **repeat**

$$\mathbf{y}_m = \text{prox}_g(\mathbf{u}_m + \mathbf{p}_m)$$

$$\mathbf{p}_{m+1} = \mathbf{u}_m + \mathbf{p}_m - \mathbf{y}_m$$

$$\mathbf{u}_{m+1} = \text{prox}_f(\mathbf{y}_m + \mathbf{q}_m)$$

$$\mathbf{q}_{m+1} = \mathbf{y}_m + \mathbf{q}_m - \mathbf{u}_{m+1}$$

until convergence

APPENDIX D: MAJORIZATION-MINIMIZATION (MM) ALGORITHMS AND A PROOF OF PROPOSITION 5.1

Recall that in the model selection problem we seek the minimizer of the following validation objective

$$\tilde{F}_\gamma(\mathbf{U}) = \frac{1}{2} \|\mathcal{P}_{\Theta^c}(\mathbf{X}) - \mathcal{P}_{\Theta^c}(\mathbf{U})\|_{\mathbb{F}}^2 + \gamma J(\mathbf{U}).$$

In this appendix, we elaborate on how to extend COBRA via a Majorization-Minimization (MM) algorithm to handle missing data in order to solve (5.1).

We begin with a brief review of MM algorithms. The basic strategy behind an MM algorithm is to convert a hard optimization problem into a sequence of simpler ones. The MM principle requires majorizing the objective function $f(\mathbf{u})$ by a surrogate function $g(\mathbf{u} | \tilde{\mathbf{u}})$ anchored at the current point $\tilde{\mathbf{u}}$. Majorization is a combination of the tangency condition $g(\tilde{\mathbf{u}} | \tilde{\mathbf{u}}) = f(\tilde{\mathbf{u}})$ and the domination condition $g(\mathbf{u} | \tilde{\mathbf{u}}) \geq f(\mathbf{u})$ for all $\mathbf{u} \in \mathbb{R}^n$. The associated MM algorithm is defined by the iterates $\mathbf{u}^{(m+1)} := \arg \min_{\mathbf{u}} g(\mathbf{u} | \mathbf{u}^{(m)})$.

It is straightforward to verify that the MM iterates generate a descent algorithm driving the objective function downhill, namely that $f(\mathbf{u}^{(m+1)}) \leq f(\mathbf{u}^{(m)})$ for all m .

Returning to our original problem, we observe that the following quadratic function of \mathbf{U} is always nonnegative

$$(D.1) \quad \frac{1}{2} \sum_{(i,j) \in \Theta} (u_{ij} - \tilde{u}_{ij})^2 \geq 0,$$

and that the inequality becomes equality when $\mathbf{U} = \tilde{\mathbf{U}}$. Adding the quadratic function in (D.1) to $\tilde{F}_\gamma(\mathbf{U})$ gives us the following function

$$\begin{aligned} g(\mathbf{U} | \tilde{\mathbf{U}}) &= \tilde{F}_\gamma(\mathbf{U}) + \frac{1}{2} \sum_{(i,j) \in \Theta} (u_{ij} - \tilde{u}_{ij})^2 \\ &= \frac{1}{2} \left[\sum_{(i,j) \in \Theta^c} (x_{ij} - u_{ij})^2 + \sum_{(i,j) \in \Theta} (u_{ij} - \tilde{u}_{ij})^2 \right] + \gamma J(\mathbf{U}) \\ &= \frac{1}{2} \|\mathbf{M} - \mathbf{U}\|_{\mathbb{F}}^2 + \gamma J(\mathbf{U}), \end{aligned}$$

where $\mathbf{M} = \mathcal{P}_{\Theta^c}(\mathbf{X}) + \mathcal{P}_{\Theta}(\tilde{\mathbf{U}})$. The function $g(\mathbf{U} | \tilde{\mathbf{U}})$ majorizes $\tilde{F}_\gamma(\mathbf{U})$ at the point $\tilde{\mathbf{U}}$, since $g(\mathbf{U} | \tilde{\mathbf{U}}) \geq \tilde{F}_\gamma(\mathbf{U})$ for all \mathbf{U} and $g(\tilde{\mathbf{U}} | \tilde{\mathbf{U}}) = \tilde{F}_\gamma(\tilde{\mathbf{U}})$. Minimizing the majorization $g(\mathbf{U} | \tilde{\mathbf{U}})$ can be accomplished by invoking COBRA on the complete matrix \mathbf{M} . Alternating between updating the majorization and applying COBRA to minimize the new majorization yields Algorithm 2 in the paper.

Having derived the majorization being minimized in [Algorithm 2](#), we are almost ready to prove [Proposition 5.1](#). We need one more ingredient. The convergence theory of monotonically decreasing algorithms, like the MM algorithm, hinges on the properties of the map $\psi(\mathbf{U})$ which returns the next iterate given the last iterate. For easy reference, we state a simple version of Meyer’s monotone convergence theorem ([Meyer, 1976](#)) which is the key ingredient in proving convergence in our setting.

THEOREM D.1. *Let $f(\mathbf{U})$ be a continuous function on a compact domain S and $\psi(\mathbf{U})$ be a continuous map from S into S satisfying $f(\psi(\mathbf{U})) < f(\mathbf{U})$ for all $\mathbf{U} \in S$ with $\psi(\mathbf{U}) \neq \mathbf{U}$. Then all limit points are fixed points of $\psi(\mathbf{U})$.*

We now prove [Proposition 5.1](#).

PROOF. We first use the above theorem to establish that the iterates of the MM algorithm tend towards the fixed points of the corresponding map, $\psi(\tilde{\mathbf{U}}) = \arg \min_{\mathbf{U}} g(\mathbf{U} | \tilde{\mathbf{U}})$. Fix an arbitrary starting guess $\mathbf{U}^{(0)}$. Set $S = \{\mathbf{U} : g(\mathbf{U} | \mathbf{U}^{(0)}) \leq F_\gamma(\mathbf{U}^{(0)})\}$. Since $g(\mathbf{U} | \mathbf{U}^{(0)})$ is continuous and coercive in \mathbf{U} , it follows that S is compact. Since $g(\mathbf{U} | \tilde{\mathbf{U}})$ is strongly convex in \mathbf{U} it follows that if $\tilde{\mathbf{U}}$ is not a fixed point then it is not the unique global minimizer of $g(\mathbf{U} | \tilde{\mathbf{U}})$ and therefore $F_\gamma(\psi(\tilde{\mathbf{U}})) < F_\gamma(\tilde{\mathbf{U}})$. By [Theorem D.1](#) the limit points of the sequence $\mathbf{U}^{(n)}$ are fixed points of $\psi(\mathbf{U})$.

We argue that the fixed points of $\psi(\mathbf{U})$ are global minimizers of the validation objective [\(5.1\)](#). Note that the mapping $\tilde{\mathbf{U}} \mapsto \psi(\tilde{\mathbf{U}})$ is characterized by the condition

$$\psi(\tilde{\mathbf{U}}) - \mathcal{P}_{\Theta^c}(\mathbf{X}) - \mathcal{P}_\Theta(\tilde{\mathbf{U}}) \in \gamma \partial J(\psi(\tilde{\mathbf{U}})).$$

If $\tilde{\mathbf{U}}$ is a fixed point of ψ then $\tilde{\mathbf{U}} = \psi(\tilde{\mathbf{U}})$, and the above optimality condition becomes

$$\mathcal{P}_{\Theta^c}(\tilde{\mathbf{U}}) - \mathcal{P}_{\Theta^c}(\mathbf{X}) \in \gamma \partial J(\tilde{\mathbf{U}}).$$

But this implies that $\tilde{\mathbf{U}}$ is a global minimizer of the validation objective [\(5.1\)](#).

Putting everything together, we have that the limit points of the MM sequence $\mathbf{U}^{(m)}$ are global minimizers of the validation objective. \square

Note that there might be infinitely many limit points. The set of limit points, however, must be contained in S and is therefore bounded. It must also be convex and closed.

As a final remark, we point out that we obtain essentially the same MM algorithm, if we substitute the objective $\tilde{F}_\gamma(\mathbf{U})$ with the objective

$$(D.2) \quad \frac{1}{2} \|\mathcal{P}_{\Theta^c}(\mathbf{X}) - \mathcal{P}_{\Theta^c}(\mathbf{U})\|_F^2 + \gamma \|\mathbf{U}\|_*,$$

where $\|\mathbf{U}\|_*$ denotes the nuclear norm of \mathbf{U} . When we substitute $\|\mathbf{U}\|_*$ for $J(\mathbf{U})$, the resulting MM algorithm is the soft-impute algorithm of [Mazumder, Hastie and Tibshirani \(2010\)](#).

APPENDIX E: SIMULATION: OVERLAPPING MULTIPLICATIVE BICLUSTERS

To test the limits of COBRA’s ability to handle model misspecification, we consider a more serious violation of the checkerboard means assumption than the one considered in [Section 6.2](#) in the paper. We replicate an example of a pair of overlapping multiplicative

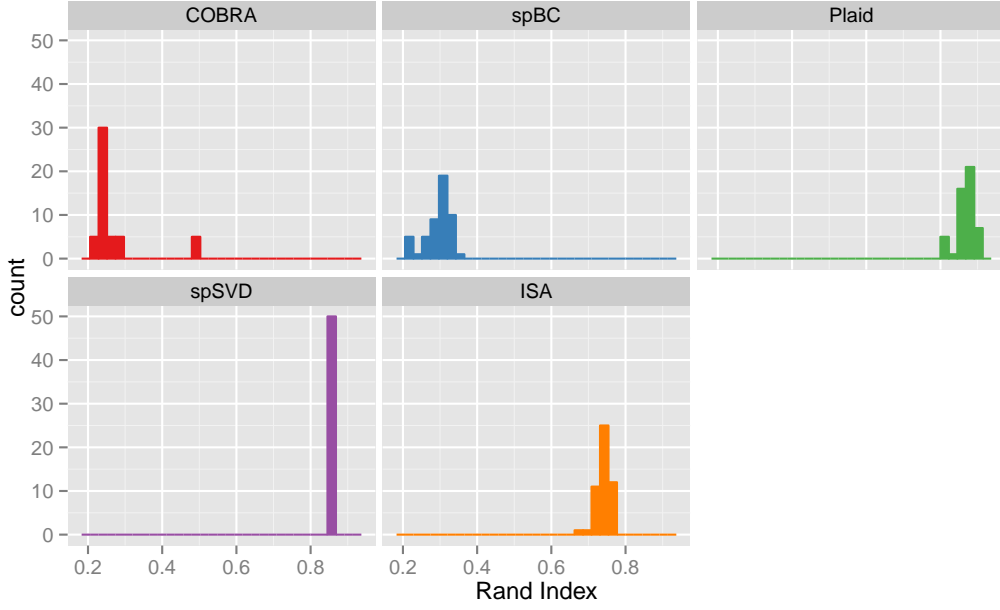


Fig 6: Pair of overlapping multiplicative means with additive iid standard normal noise. Each panel shows the histogram of the Rand index of estimated and true support (union of the pair of biclusters) for the convex biclustering algorithm (COBRA), sparse biclustering (spBC), Plaid model, sparse SVD (spSVD), and iterative signature algorithm (ISA).

biclusters from [Lee et al. \(2010\)](#) and [Tan and Witten \(2013\)](#). The underlying means matrix is given by $\mathbf{M} = d\mathbf{u}_1\mathbf{v}_1^\top + d\mathbf{u}_2\mathbf{v}_2^\top$ where $d = 50$, and

$$\begin{aligned}\tilde{\mathbf{u}}_1 &= (10 \ 9 \ 8 \ 7 \ 6 \ 5 \ 4 \ 3 \ \text{rep}(2, 17) \ \text{rep}(0, 75))^\top, \\ \tilde{\mathbf{v}}_1 &= (10 \ -10 \ 8 \ -8 \ 5 \ -5 \ \text{rep}(-3, 5) \ \text{rep}(0, 34))^\top, \\ \tilde{\mathbf{u}}_2 &= (\text{rep}(0, 13) \ 10 \ 9 \ 8 \ 7 \ 6 \ 5 \ 4 \ 3 \ \text{rep}(2, 17) \ \text{rep}(0, 62))^\top, \\ \tilde{\mathbf{v}}_2 &= (\text{rep}(0, 9) \ 10 \ -9 \ 8 \ -7 \ 6 \ -5 \ \text{rep}(4, 5) \ \text{rep}(-3, 5) \ \text{rep}(0, 25))^\top,\end{aligned}$$

where $\text{rep}(a, b)$ denotes a vector of length b whose entries are all a . The means matrix is computed using the normalized vectors $\mathbf{u} = \tilde{\mathbf{u}}/\|\tilde{\mathbf{u}}\|_2$ and $\mathbf{v} = \tilde{\mathbf{v}}/\|\tilde{\mathbf{v}}\|_2$. The data matrix is given by $\mathbf{X} = \mathbf{M} + \boldsymbol{\varepsilon}$, where $\varepsilon_{ij} \sim \text{iid } \mathcal{N}(0, 1)$. We partition the set of indices into two groups, the union of the two bicluster support and its complement. [Figure 6](#) shows the boxplots of the Rand index of 50 replicates. The Rand index is computed between the true bicluster support and the biclusterings obtained by COBRA, spBC, and the bicluster support obtained by Plaid, spSVD, and ISA.

Both COBRA and spBC struggle with the non-checkerboard structure. As noted in [Tan and Witten \(2013\)](#), however, adding a sparsity penalty can improve the support recovery in this context. In fact, they empirically show that overlapping multiplicative biclusters can be approximated as the union of a collection of constant biclusters and that with a judiciously chosen amount of ℓ_1 penalization, a sparse checkerboard mean structure can do admirably in recovering the support. While this result is encouraging, it remains unclear how to automatically choose the amount of ℓ_1 penalization. Indeed, their

BIC method for selecting the amount of ℓ_1 regularization tends to recover supports that are too dense. While spBC and COBRA are not intended to recover non-checkerboard mean structure, it remains an intriguing avenue of future research to determine how these methods may be refined to gracefully deal with such model-misspecification automatically. Finally, we note that although the data matches the generating mechanism for spSVD, it does not always perform the best. One has to take into account that we used stability selection to choose the tuning parameters and in general selection of tuning parameters can be quite challenging.

REFERENCES

- BAUSCHKE, H. H. and COMBETTES, P. L. (2008). A Dykstra-like algorithm for two monotone operators. *Pacific Journal of Optimization* **4** 383–391.
- BERGMANN, S., IHMELS, J. and BARKAI, N. (2003). Iterative signature algorithm for the analysis of large-scale gene expression data. *Physical review E* **67** 031902.
- BOYD, S., PARIKH, N., CHU, E., PELEATO, B. and ECKSTEIN, J. (2011). Distributed Optimization and Statistical Learning via the Alternating Direction Method of Multipliers. *Foundations and Trends in Machine Learning* **3** 1–122.
- BOYLE, J. P. and DYKSTRA, R. L. (1986). A Method for Finding Projections onto the Intersection of Convex Sets in Hilbert Spaces. In *Advances in Order Restricted Statistical Inference*, (R. Dykstra, T. Robertson and F. T. Wright, eds.). *Lecture Notes in Statistics* **37** 28–47. Springer New York.
- BUSYGIN, S., PROKOPYEV, O. and PARDALOS, P. M. (2008). Biclustering in data mining. *Computers and Operations Research* **35** 2964–2987. Part Special Issue: Bio-inspired Methods in Combinatorial Optimization.
- CHENG, Y. and CHURCH, G. M. (2000). Biclustering of expression data. In *Proceedings of the 8th International Conference of Intelligent Systems and Molecular Biology* **8** 93–103.
- CHI, E. C. and LANGE, K. (2014). Splitting Methods for Convex Clustering. *Journal of Computational and Graphical Statistics*. in press.
- CHI, E. C., ZHOU, H., CHEN, G. K., VECCHYO, D. O. and LANGE, K. (2013). Genotype Imputation via Matrix Completion. *Genome Research* **23** 509–518.
- COIFMAN, R. R. and GAVISH, M. (2011). Harmonic Analysis of Digital Data Bases. In *Wavelets and Multiscale Analysis*, (J. Cohen and A. I. Zayed, eds.). *Applied and Numerical Harmonic Analysis* 161–197. Birkhäuser Boston.
- COMBETTES, P. L. and PESQUET, J.-C. (2011). Proximal Splitting Methods in Signal Processing. In *Fixed-Point Algorithms for Inverse Problems in Science and Engineering*, (H. H. Bauschke, R. S. Bucrak, P. L. Combettes, V. Elser, D. R. Luke and H. Wolkowicz, eds.). *Springer Optimization and Its Applications* 185–212. Springer New York.
- DEO, N. (1974). *Graph Theory with Applications to Engineering and Computer Science*. Prentice-Hall, Inc., Upper Saddle River, NJ, USA.
- DEUTSCH, F. (1992). The Method of Alternating Orthogonal Projections. In *Approximation Theory, Spline Functions and Applications*, (S. P. Singh, ed.). *NATO ASI Series* **356** 105–121. Springer Netherlands.
- DHILLON, I. S. (2001). Co-clustering documents and words using bipartite spectral graph partitioning. In *Proceedings of the Seventh ACM SIGKDD International Conference on Knowledge Discovery and Data Mining* 269–274.
- DYKSTRA, R. L. (1983). An Algorithm for Restricted Least Squares Regression. *Journal of the American Statistical Association* **78** 837–842.
- FRIEDMAN, J., HASTIE, T., HÖFLING, H. and TIBSHIRANI, R. (2007). Pathwise coordinate optimization. *Annals of Applied Statistics* **1** 302–332.
- HASTIE, T., TIBSHIRANI, R. and FRIEDMAN, J. (2009). *The Elements of Statistical Learning: Data Mining, Inference, and Prediction, Second Edition*. *Springer Series in Statistics*. Springer.
- HOCKING, T., VERT, J.-P., BACH, F. and JOULIN, A. (2011). Clusterpath: an Algorithm for Clustering using Convex Fusion Penalties. In *Proceedings of the 28th International Conference on Machine Learning (ICML-11)* (L. Getoor and T. Scheffer, eds.). *ICML '11* 745–752. ACM, New York, NY, USA.
- HOFMANN, T. and PUZICHA, J. (1999). Latent Class Models for Collaborative Filtering. In *Proceedings of the Sixteenth International Joint Conference on Artificial Intelligence. IJCAI '99* 688–693. Morgan Kaufmann Publishers Inc., San Francisco, CA, USA.
- KLUGER, Y., BASRI, R., CHANG, J. T. and GERSTEIN, M. (2003). Spectral Biclustering of Microarray Data: Coclustering Genes and Conditions. *Genome Research* **13** 703–716.

- LANGE, K. (2013). *Optimization*, 2nd ed. *Springer Texts in Statistics* **95**. Springer.
- LANGE, K., HUNTER, D. R. and YANG, I. (2000). Optimization Transfer Using Surrogate Objective Functions (with discussion). *Journal of Computational and Graphical Statistics* **9** 1–20.
- LAZZERONI, L. and OWEN, A. (2002). Plaid Models for Gene Expression Data. *Statistica Sinica* **12** 61–86.
- LEE, M., SHEN, H., HUANG, J. Z. and MARRON, J. S. (2010). Biclustering via Sparse Singular Value Decomposition. *Biometrics* **66** 1087–1095.
- LINDSTEN, F., OHLSSON, H. and LJUNG, L. (2011). Just Relax and Come Clustering! A Convexification of k -Means Clustering Technical Report, Linköpings Universitet.
- LIU, Y., HAYES, D. N., NOBEL, A. and MARRON, J. S. (2008). Statistical Significance of Clustering for High-Dimension, Low-Sample Size Data. *Journal of the American Statistical Association* **103** 1281–1293.
- MADEIRA, S. C. and OLIVEIRA, A. L. (2004). Biclustering algorithms for biological data analysis: A survey. *Computational Biology and Bioinformatics, IEEE/ACM Transactions on* **1** 24–45.
- MAZUMDER, R., HASTIE, T. and TIBSHIRANI, R. (2010). Spectral Regularization Algorithms for Learning Large Incomplete Matrices. *Journal of Machine Learning Research* **11** 2287–2322.
- MEINSHAUSEN, N. (2007). Relaxed Lasso. *Computational Statistics and Data Analysis* **52** 374–393.
- MEYER, R. R. (1976). Sufficient conditions for the convergence of monotonic mathematical programming algorithms. *Journal of Computer and System Sciences* **12** 108–121.
- PAN, W., SHEN, X. and LIU, B. (2013). Cluster Analysis: Unsupervised Learning via Supervised Learning with a Non-convex Penalty. *Journal of Machine Learning Research* **14** 1865–1889.
- PELCKMANS, K., DE BRABANTER, J., SUYKENS, J. and DE MOOR, B. (2005). Convex clustering shrinkage. In *PASCAL Workshop on Statistics and Optimization of Clustering Workshop*.
- RAND, W. M. (1971). Objective Criteria for the Evaluation of Clustering Methods. *Journal of the American Statistical Association* **66** 846–850.
- SHABALIN, A. A., WEIGMAN, V. J., PEROU, C. M. and NOBEL, A. B. (2009). Finding large average submatrices in high dimensional data. *Annals of Applied Statistics* **3** 985–1012.
- SILL, M., KAISER, S., BENNER, A. and KOPP-SCHNEIDER, A. (2011). Robust biclustering by sparse singular value decomposition incorporating stability selection. *Bioinformatics* **27** 2089–2097.
- SØRLIE, T., PEROU, C. M., TIBSHIRANI, R., AAS, T., GEISLER, S., JOHNSEN, H., HASTIE, T., EISEN, M. B., VAN DE RIJN, M., JEFFREY, S. S. et al. (2001). Gene expression patterns of breast carcinomas distinguish tumor subclasses with clinical implications. *Proceedings of the National Academy of Sciences* **98** 10869–10874.
- SØRLIE, T., TIBSHIRANI, R., PARKER, J., HASTIE, T., MARRON, J., NOBEL, A., DENG, S., JOHNSEN, H., PESICH, R., GEISLER, S. et al. (2003). Repeated observation of breast tumor subtypes in independent gene expression data sets. *Proceedings of the National Academy of Sciences* **100** 8418–8423.
- TAN, K. M. and WITTEN, D. M. (2013). Sparse Biclustering of Transposable Data. *Journal of Computational and Graphical Statistics*. in press.
- TANAY, A., SHARAN, R. and SHAMIR, R. (2005). *Handbook of computational molecular biology. Computer and Information Science Series* **9** Biclustering algorithms: A survey. Chapman and Hall/CRC.
- TIBSHIRANI, R. (1996). Regression Shrinkage and Selection via the Lasso. *Journal of the Royal Statistical Society: Series B (Statistical Methodology)* **58** 267–288.
- TIBSHIRANI, R. J. and TAYLOR, J. (2011). The solution path of the generalized Lasso. *Annals of Statistics* **39** 1335–1371.
- TIBSHIRANI, R., SAUNDERS, M., ROSSET, S., ZHU, J. and KNIGHT, K. (2005). Sparsity and smoothness via the fused Lasso. *Journal of the Royal Statistical Society: Series B (Statistical Methodology)* **67** 91–108.
- TOTHILL, R. W., TINKER, A. V., GEORGE, J., BROWN, R., FOX, S. B., LADE, S., JOHNSON, D. S., TRIVETT, M. K., ETEMADMOGHADAM, D., LOCANDRO, B. et al. (2008). Novel molecular subtypes of serous and endometrioid ovarian cancer linked to clinical outcome. *Clinical Cancer Research* **14** 5198–5208.
- TURNER, H., BAILEY, T. and KRZANOWSKI, W. (2005). Improved biclustering of microarray data demonstrated through systematic performance tests. *Computational Statistics and Data Analysis* **48** 235–254.
- WITTEN, D. M., TIBSHIRANI, R. and HASTIE, T. (2009). A penalized matrix decomposition, with applications to sparse principal components and canonical correlation analysis. *Biostatistics* **10** 515–534.
- WOLD, S. (1978). Cross-Validatory Estimation of the Number of Components in Factor and Principal Components Models. *Technometrics* **20** 397–405.
- WU, T. T. and LANGE, K. (2008). Coordinate Descent Algorithms for Lasso Penalized Regression. *Annals of Applied Statistics* **2** 224–244.

E. C. CHI
DEPARTMENT OF ELECTRICAL
AND COMPUTER ENGINEERING
RICE UNIVERSITY
HOUSTON, TX 77005
USA
E-MAIL: echi@rice.edu

G. I. ALLEN
DEPARTMENT OF STATISTICS
RICE UNIVERSITY
HOUSTON, TX 77005
USA
E-MAIL: gallen@rice.edu

R. G. BARANIUK
DEPARTMENT OF ELECTRICAL
AND COMPUTER ENGINEERING
RICE UNIVERSITY
HOUSTON, TX 77005
USA
E-MAIL: richb@rice.edu